PATTERNS OF CARBON DIOXIDE AND WATER VAPOR FLUX FOLLOWING HARVEST OF TALLGRASS PRAIRIE AT DIFFERENT TIMES THROUGHOUT THE GROWING SEASON

by

JOHN THOMAS MURPHY

B.S., Central Missouri State University, 2002

M.S., South Dakota State University, 2004

AN ABSTRACT OF A DISSERTATION

submitted in partial fulfillment of the requirements for the degree

DOCTOR OF PHILOSOPHY

Department Of Agronomy

College of Agriculture

KANSAS STATE UNIVERSITY

Manhattan, Kansas

2007

Abstract

Most rangelands are harvested at some point during the year and removal of plant leaf area and biomass alters a host of ecosystem processes including gas exchange. An experiment was conducted in 2005 and 2006 to study the effects of clipping tallgrass prairie at different dates on water vapor and CO_2 fluxes. A portable, non-steady-state chamber was designed to measure CO_2 and water vapor fluxes from small plots in less than 40 s. A combination of sunlit and shaded readings allowed measurements of net carbon exchange (NCE) and ecosystem respiration (R_E); by summing NCE and R_E, gross canopy photosynthesis (GCP) was calculated. Throughout the two-year study, the chamber had a minimal effect on microclimate, i.e., average chamber temperature increased 2.9° C, while chamber pressure increased only 0.3 Pa during measurements, and photosynthetically active radiation attenuation was 10%. The immediate effect of all clipping treatments was a loss of leaf area that led to reductions in GCP, NCE, and R_E and in most cases decreased water vapor flux. Further patterns of carbon flux were governed by the amount of water stress during canopy development, while water vapor flux rates varied with water availability. Canopies that developed during periods of low water stress quickly increased carbon flux rates following precipitation after a mid-season drought. However, flux rates of canopies, which developed during the mid-season drought, responded considerably slower to subsequent water availability. A separate experiment was conducted from June-October of 2006 to estimate GCP, leaf area index (LAI), and total aboveground biomass with a hyperspectral radiometer. Indices such as the Normalized Difference Vegetation Index and the Simple Ratio were used to estimate LAI and biomass had

poor correlations with measured values. However, GCP was significantly correlated to all six indices derived in this study. While GCP measured from June-October was significantly correlated with all indices, removal of the senesced canopy scans recorded during October greatly increased the relationship.

PATTERNS OF CARBON DIOXIDE AND WATER VAPOR FLUX FOLLOWING HARVEST OF TALLGRASS PRAIRIE AT DIFFERENT TIMES THROUGHOUT THE GROWING SEASON

by

JOHN THOMAS MURPHY

B.S., Central Missouri State University, 2002
M.S., South Dakota State University, 2004

A DISSERTATION

submitted in partial fulfillment of the requirements for the degree

DOCTOR OF PHILOSOPHY

Department Of Agronomy
College of Agriculture

KANSAS STATE UNIVERSITY
Manhattan, Kansas

2007

Approved by:

Major Professor
Clenton Owensby, Ph.D.

Copyright

Abstract

Most rangelands are harvested at some point during the year and removal of plant leaf area and biomass alters a host of ecosystem processes including gas exchange. An experiment was conducted in 2005 and 2006 to study the effects of clipping tallgrass prairie at different dates on water vapor and CO_2 fluxes. A portable, non-steady-state chamber was designed to measure CO_2 and water vapor fluxes from small plots in less than 40 s. A combination of sunlit and shaded readings allowed measurements of net carbon exchange (NCE) and ecosystem respiration (R_E); by summing NCE and R_E, gross canopy photosynthesis (GCP) was calculated. Throughout the two-year study, the chamber had a minimal effect on microclimate, i.e., average chamber temperature increased 2.9° C, while chamber pressure increased only 0.3 Pa during measurements, and photosynthetically active radiation attenuation was 10%. The immediate effect of all clipping treatments was a loss of leaf area that led to reductions in GCP, NCE, and R_E and in most cases decreased water vapor flux. Further patterns of carbon flux were governed by the amount of water stress during canopy development, while water vapor flux rates varied with water availability. Canopies that developed during periods of low water stress quickly increased carbon flux rates following precipitation after a mid-season drought. However, flux rates of canopies, which developed during the mid-season drought, responded considerably slower to subsequent water availability. A separate experiment was conducted from June-October of 2006 to estimate GCP, leaf area index (LAI), and total aboveground biomass with a hyperspectral radiometer. Indices such as the Normalized Difference

Vegetation Index and the Simple Ratio were used to estimate LAI and biomass had poor correlations with measured values. However, GCP was significantly correlated to all six indices derived in this study. While GCP measured from June-October was significantly correlated with all indices, removal of the senesced canopy scans recorded during October greatly increased the relationship.

Table of Contents

List of Figures

List of Tables

Acknowledgements

I am indebted to Dr. Clenton Owensby and Dr. Jay Ham for their guidance, support, and friendship during the past three years. I would also like to acknowledge my Ph.D. committee, Dr. Patrick Coyne, Dr. John Blair, and Dr. Ronaldo Maghirang for their support, advice, and help. I am also grateful to Dr. George Milliken for his statistical consulting.

A much deserved thank-you to my fellow graduate student Jamey Duesterhaus is also due. I appreciate his friendship and always-available, helping attitude. Jamey helped me with every day of data collection and logistical problems throughout this study. I also appreciate the help of Lisa Auen. I also acknowledge the help with chamber fabrication and general maintenance of Mr. Fred Caldwell.

I must dedicate this dissertation to my family, without them I would never have accomplished this. My wife Katie and two sons, Dan and Andrew, have been a constant source of laughter, love, strength, and sanity during this process. I also need to thank my Mom and Dad. They have been and continue to be a source of encouragement, love, and support for my family and me. Lastly, I would like to thank both of my sisters, Sarah and MaryKate, for their laughter and listening and caring hearts. Thank-you!

CHAPTER 1 - Design of a Novel Gas Exchange Chamber

Abstract

Removal of rangeland vegetation by grazing alters a host of ecosystem processes including carbon and water vapor flux rates. Measurement of those flux rates enhances the understanding of ecosystem processes. A transparent closed-system, non-steady-state chamber was developed that allowed measurements of net carbon exchange (NCE) when sunlit and ecosystem respiration (R_E) when covered by an opaque box. While other gas exchange methods (i.e., eddy correlation) have been successfully utilized on rangelands, advantages of chambers include measurements at the plot scale rather than field scale. This permits statistical designs using replicated treatments in relatively small, uniform areas. The chamber was 0.85-m x 0.85-m with a height of 0.25-m and total weight of 10.9 kg. The sides were constructed of clear Plexiglas while the top of the chamber was a heat-stretched Propafilm-C. Minimizing alterations to the chamber microclimate were of primary concern. To quantify alterations to the microclimate, the chamber was tested for two years over a range of climatic, leaf area, and biomass levels on an ungrazed tallgrass prairie near Manhattan, KS. Throughout the two years of testing, the chamber had a minimal effect on microclimate; average chamber air temperature increased 2.9° C over 40 s, while chamber pressure increased only 0.3 Pa, and photosynthetically active radiation attenuation was 10%. Also, a method for selecting the appropriate model (linear or quadratic) to calculate the rate change of CO_2 and water vapor from time-series data

collected by the chamber was developed. The method utilized a computer program that determined whether the quadratic model, based on shape of the CO_2 vs. time curve. Using this method, the quadratic flux estimate was utilized for 80.1% of all NCE flux calculations, 14.2% of the R_E flux calculations, and 99.5% of water vapor flux calculations.

Introduction

Field observations of carbon and water vapor fluxes are critical to understanding how ecosystems respond to different land management practices. Advantages of using chambers over other micrometeorological techniques (i.e. eddy correlation) include the ability to measure responses at the plot scale rather than field scale, replicate treatments in relatively small, uniform areas, and portability. Chamber portability is an essential design criterion to allow easy maneuverability among research plots. Early chamber designs were large, requiring forklifts or tractors to position or relocate them (Reicosky and Peters 1977). Recent designs have stressed lightweight materials that are manipulated more easily (Risch and Frank 2006). However, chambers can alter the microclimate and architecture of the canopy.

Microclimate perturbations caused by chambers have been well addressed in the literature and include the creation of pressure gradients and alteration of CO_2 gradients, turbulence regimes, air and leaf temperatures, radiation attenuation, and vapor pressure deficit (Wagner and Reicosky 1992, Steduto et al. 2002, Bremer and Ham 2005). Alterations to the chamber microenvironment are the main objections to using closed chamber methods. Minimizing microclimate modifications within the chamber has been accomplished by actively controlling air temperature and humidity within the chamber (Wilsey et al. 2002) and by performing measurements of short duration (Steduto et al. 2002).

When using the non-steady state method, the rate of change in concentration of CO_2 ($\delta CO_2/\delta t$) and water vapor ($\delta wc/\delta t$) must be calculated to estimate gas exchange. Both linear and quadratic models have been used to calculate $\delta CO_2/\delta t$ and $\delta wc/\delta t$

(Wagner et al. 1997, Steduto et al. 2002). Wagner and Reicosky (1992) found that even when r^2>0.97, CO_2 flux was underestimated by 10%. Wagner et al. (1997) reported an average difference of 47% between linear and quadratic evapotranspiration calculations. In non-steady state systems, Wagner et al. (1997) and Studeto et al. (2002) stated that the quadratic model could be considered the most effective. Furthermore, a non-linear least squares method is utilized for calculating fluxes from data collected by the LI-8100 (LiCor 2007). The goal with each model is to calculate the slope of $\delta CO_2/\delta t$ and $\delta wc/\delta t$ at the moment chamber conditions approximate ambient or before the chamber has significantly changed canopy microclimate (i.e., the very start of the measurement, t=0).

Other chamber designs have been utilized on rangelands (Angell and Svejcar 1999, Wilsey et al. 2002, Risch and Frank 2006). However, some of the chambers are designed to remain on the plot being vented by doors between readings and are heavy (> 20 kg) while other chambers are climate-controlled, but remain on the plot for up to 180 s during a reading. An objective of this research was to design and fabricate a lightweight, portable chamber to measure CO_2 and water vapor fluxes of rangeland in a closed, non-steady-state environment with minimal alterations to canopy microclimate. A transparent chamber was used to measure net carbon exchange (NCE) in the light and a tight fitting opaque box was placed over the chamber to measure ecosystem respiration (R_E) in the dark. Field testing examined: 1) how quickly could measurements be made, 2) what was the temperature, pressure, vapor pressure deficits (VPD), and light effects, and 3) what types of correction for leaks and the build up of water vapor are required. Another objective was to develop a method of selecting

the most appropriate model (linear or quadratic) to calculate CO_2 and water vapor fluxes.

Chamber Design

The chamber sample area was 0.85-m x 0.85-m with a height of 0.25-m and total weight of 10.9 kg. Sides were constructed of 4.59-mm acrylic-FE (Acrylite, Cyro Industries, Clifton, NJ) (Fig. 1.1). The top was made from heat-stretched Propafilm-C (ICI Americas Inc., Wilmington, DE) with high thermal and visible transmittance (Hunt 2003). A closed-cell foam gasket (Nomapack-WS, Nomaco Inc, Zebulon, NC) provided a tight seal between the bottom edges of the chamber sides and the soil collar. The soil collars were constructed of 5.1 cm x 7.6 cm x 0.5 cm angle iron that were pressed into the soil until 5 cm was exposed above ground. Two fans (700 L min^{-1}, BD 12A3, Comair Rotron, San Diego, CA) circulated air through a perforated plenum that was attached near the base of the entire chamber. The plenum was 2.1 cm x 4.3 cm electric raceway (PN10L08V, Wiremold, West Hartford, CT) with two rows of 1.8 mm holes drilled 1.3 cm from the top and bottom of the raceway and spaced 1.3 cm apart. Two additional fans (V571M, Micronel, Fallbrook, CA) were positioned near the top of the chamber, opposite the Comair fans, to promote heat transfer across the propafilm and increase air mixing. Four vents 0.25-m long by 14.3-mm inside diameter were installed on the chamber walls to equilibrate chamber and atmosphere pressure.

A closed path infrared gas analyzer (IRGA, LI-840, Li-Cor Industries, Lincoln, NE) was used to measure CO_2 and water vapor concentrations every second during a test. A continuous air sample was supplied to the IRGA at 1.0 L min^{-1} by a rotary pump (model 50095, Thomas Pumps, Sheboygan, WI); rotary pumps minimize pressure

fluctuations in the optical bench of the IRGA. Air was sampled from the plenum to obtain a well-mixed sample. A 0.4-mm-diameter thermistor (10K3MCD1, Betatherm Corp., Shrewburg, MA) placed inside the plenum, 5 cm below one of the Comair Rotron fans, measured chamber air temperature. Photosynthetically active radiation (PAR) flux was measured outside the chamber with a quantum sensor (LI-190, Li-Cor Inc.). A CR10X (Campbell Scientific, Logan, UT) logged data from all instruments at 1 Hz. Both the IRGA and CR10X were mounted on a 3.2-mm-thick aluminum plate that was painted flat gray. A sun shield was mounted over the top of the instruments to further shield the instruments from radiation. The system was powered by a 12-V, 12 amp-hr battery, which could run the chamber for 2 hours after a full charge.

Field Setup

The chamber was tested in an ungrazed, annually burned pasture located in the Rannells Flint Hills Prairie Preserve, 5 km south of Manhattan, KS (39.11°N, 96.34°W, 324 m above sea level) that was burned during the last 10 days of April. The dominant vegetation consisted of the native C_4 species *Andropogon gerardii* Vitman and *Sorghastrum nutans* (L.) Nash while subdominants included *A. scoparius* Michx. and *Bouteloua curtipendula* (Michx.) Kunth. The remainder of the vegetation consisted of various sedges (C_3), and C_3 forbs including *Vernonia baldwinii* (Small) Schub., *Ambrosia psilostachya* DC., *Artemesia ludoviciana* Nutt., and *Psorelea tenuiflora* var. *floribunda* (Nutt.) Rydb. The soil was a Dwight silty clay (Fine, smectitic, mesic Typic Natrustolls) on a 1-3% slope. Average annual precipitation (1971-2000) was 884 mm with 542 mm occurring from May through September.

Eighteen plots, 0.85 m x 0.85 m, were established in mid-May of 2005 and 2006. At six different dates during June through August, three of the plots were clipped, resulting in the chamber being used over a wide range of canopy sizes and biomass levels. Net carbon exchange was measured with the chamber exposed to ambient light. All readings occurred between 1030-1500 (DST) during clear days. Readings were taken on 24 dates between June to September and June to October in 2005 and 2006. Chamber measurements were initiated by recording ambient conditions above the canopy for 20 seconds. Data acquisition was then paused for five seconds while the chamber was positioned over the canopy and placed onto the soil frame. Following the five-second pause, data acquisition resumed for a 40-second period with the chamber positioned over the canopy. Following each reading, the chamber was removed from the canopy and the CO_2 and water vapor concentrations and air temperature within the chamber were allowed to equilibrate with ambient conditions.

Environmental Tests

Leak Test

Considerable effort was made in the design and fabrication of the chamber to minimize entry of ambient air into the chamber. The sheets of Plexiglas that formed the chamber walls were fused with trichloroethylene and further sealed with silicone at each joint. The Propafilm top was sealed to the chamber walls with clear packing tape. However, completely eliminating the exchange of air between the chamber and the ambient environment was extremely difficult. To quantify this potential source of error in the flux calculations, leak tests were conducted prior to each sampling date. This test

consisted of positioning the chamber on a flat aluminum surface, in the field, and injecting 24 ml of pure CO_2 into the chamber to create a CO_2 concentration gradient >100 $\mu l\ l^{-1}$ across the chamber walls. This gradient is considerably greater than those created during normal chamber readings (average measurement gradient was typically 35 $\mu l\ l^{-1}$). The gradual decrease of CO_2 within the chamber was monitored and used to calculate a leakage rate of CO_2 from the chamber. The CO_2 leakage rates averaged 0.12 ± 0.005 $\mu mol\ m^{-2}\ s^{-1}$ (mean $\pm$ SE, n=261) and 0.09 ± 0.02 $\mu mol\ m^{-2}\ s^{-1}$ (n=401) over the 2005 and 2006 growing seasons, respectively. These rates were considered negligible and the final flux calculations were not corrected for leaks.

Pressure Test

Increased pressure within a chamber has the ability to partially suppress the efflux of CO_2 from the soil, which could create an artificially high net canopy CO_2 flux (Owensby et al. 1997, Lund et al. 1999, Bremer and Ham 2005). Because the chamber is operated in a closed state, pressure increases could result from either air handling or evapotranspiration (ET). Air moving over the soil surface in response to the forced ventilation of the mixing fans increases pressure and chamber designs that have excessive air flow likely depress soil CO_2 flux. The perforated air plenum was designed to evenly distribute air throughout the chamber and reduce air speed. Evapotranspiration adds additional water vapor to the chamber headspace. Boyle's law predicts pressure must increase as additional gas is added to a sealed, constant volume chamber. Pressure increases were attenuated by venting the chamber to the atmosphere. The initial chamber design incorporated a single vent constructed from flexible tubing measuring 0.45-m long by 14.3-mm inside diameter. However, a

numerical model of the chamber showed that ET from large, actively growing canopies might cause pressure increases. Thus, the chamber was redesigned incorporating four vents 0.25-m long by 14.3-mm inside diameter (Ham, personal communication 2006).

Chamber pressure was measured in both the laboratory and field. In the lab, a differential pressure transducer (Furness PPC-500, Indian Trail, NC) measured pressure within the empty chamber that was placed on an elevated platform with nine sampling points positioned in a single line down the center of the chamber. The pressure transducer was connected to one of the nine sampling points and while the chamber was operated in measurement mode the pressure at each sampling point was recorded for 60 seconds. Field measurements also utilized a differential pressure transducer (Setra 264, Setra, 0 – 0.1 " H_2O range, Boxborough, MA, 01719-1304). One sampling tube was suspended near the center of the chamber approximately 50-mm above the soil surface, while the other tube was positioned outside the chamber within the grass canopy at approximately the same height.

Average chamber pressure measured in the lab was 0.58 ± 0.08 Pa (mean $\pm$ SE, n = 9) above ambient. The average chamber pressure recorded during field sampling was 0.32 ± 0.04 Pa (mean $\pm$ SE, n = 418) above ambient. This very minimal increase in chamber pressure during a reading (Fig. 1.2) was less than that reported from many other chamber designs. The venting system described above, and the perforated air plenum, minimized pressure increases caused by ET and air movement in the chamber to the extent that corrections to flux calculations were not indicated.

Temperature

Increased temperature can modify carboxylation rates by altering ribulose-1-5-bisphosphate carboxylase (Rubisco) activity (Bernacchi et al. 2002). Rubisco catalyzes the reaction that reduces CO_2 to carbohydrate during photosynthesis. Altering the rate of carboxylation directly affects measurements of NCE. One of the main reasons for attempting a short duration measurement (40 s) was to minimize heating. Throughout both years of the study, the average temperature increased 2.9 $\pm$ 0.024°C (mean $\pm$ SE, n = 883) during the 40 s sampling interval (Figure 1.3). Chamber temperature increases of 2-4°C are commonly reported in the literature (Wagner and Reicosky 1992, Steduto et al. 2002).

Photosynthetically Active Radiation Attenuation

Chamber materials were selected to minimize attenuation of photosynthetically active radiation (PAR). Photosynthetically active radiation (400-700 nm) is the driving force of photosynthesis providing energy to photosystems I and II. Artificial reductions in PAR directly affect measurements of canopy photosynthesis.

Attenuation of PAR by the chamber was determined using a 0.5 m light bar with six quantum sensors (LQS506-SUN, Apogee, Logan, UT). The measurements occurred on a level surface during a cloudless day. A detailed map of PAR attenuation was constructed by measuring PAR at 100-mm increments within the chamber beginning 20-mm from the side of the chamber opposite the IRGA. A narrow shadow, 5-mm wide, was measured at the 20-mm distance, which decreased overall transmittance (Fig. 1.4). This narrow shadow resulted from the joining of the Plexiglas sides and propafilm top. Other than the 5-mm wide shadow, the chamber design

allowed for approximately 90% PAR transmittance. The 10% attenuation by the chamber material was less than that reported by Pickering et al. (1993) and Steduto et al. (2002) of 20% and 12%, respectively. Overall, the chamber allowed for higher transmittance of PAR than that of previously reported chambers. The higher transmittance values probably derived from the use of propafilm as a top instead of Plexiglas. This result suggested that the current chamber construction minimized modifications to the PAR regime.

Examples of CO_2 and VPD rate changes

The chamber was tested over a wide range of canopy sizes and climatic conditions. Substantial rate changes of CO_2 and decreasing VPD's were associated with periods of high soil water content and large canopies (Fig. 1.5 a,b). However, the rate change of CO_2 and VPD's remained mostly unchanged during measurements on plots following removal of leaf area by clipping (Fig. 1.6 a,b).

Flux Model and Calculation

The basic formulas for computing CO_2 (J_c) and water vapor (J_w) fluxes are:

$$J_c = \rho_m \frac{V}{A} \frac{\delta CO_2}{\delta t} \qquad \text{[eq 1.1]}$$

$$J_w = \rho_m \frac{V}{A} \frac{\delta w_c}{\delta t} \qquad \text{[eq 1.2]}$$

Where J_c and J_w are flux density (mol m^{-2} s^{-1}), ρ_m is the molar density of air (mol_{air} m^{-3}_{air}) calculated from the ideal gas law, V is the chamber volume (m^3_{air}), A is the chamber area (m^2_{land}) and $\delta CO_2/\delta t$ and $\delta w_c/\delta t$ are the rate changes over time of CO_2

and water vapor concentrations within the chamber (mol $_{CO_2}$ or $_{H_2O}$ mol$^{-1}_{air}$s^{-1}) respectively (Ham et al. 2005). The calculation of J_c is corrected for water vapor dilution as follows:

$$J_c = \rho_m \frac{V}{A}\left(\frac{\delta CO_2}{\delta t} + \frac{CO_2}{(1-w_c)} \div \frac{\delta w_c}{\delta t}\right) \qquad \text{[eq 1.3]}$$

where w_c is the mole fraction of water vapor within the headspace (mol mol^{-1}) and $\delta w_c / \delta t$ is the rate change of w_c (mol mol^{-1} s^{-1}). Corrections due to water vapor dilution were substantial during the two years of the study. The average difference between corrected and uncorrected NCE fluxes was 12.9% with a maximum correction difference of 29.2%. The results indicate the significant impact of correcting for water vapor dilution in closed chambers.

Determination of Flux

The preferred models for calculating $\delta CO_2/\delta t$ and $\delta wc/\delta t$ have been discussed by Wagner and Reicosky 1992, Wagner et al. 1997, and Steduto et al. 2002. These studies mainly utilized either a linear or quadratic regression equation. The goal in selecting a model is to accurately predict flux when conditions within the closed chamber match ambient conditions, or before the chamber significantly influences the canopy environment.

A weakness of the linear model is that the rates of photosynthesis and transpiration are assumed to remain constant with decreasing concentration of CO_2 and increasing concentration of water vapor in the chamber. However, this is unlikely as shown by Fick's first law of diffusion

$$F_j = -D_j \frac{\delta c_j}{\delta x} \qquad \text{[eq 1.4]}$$

where F_j is the flux of j, D_j is the diffusion coefficient, and $\delta c_j / \delta x$ is the gradient of j between the chamber air and intercellular leaf air. This equation predicts the rate of diffusion of CO_2 into and water vapor out of the leaf will decrease as concentrations of CO_2 decrease and water vapor increase, respectively, within the chamber.

Wagner et al. (1997) and Studeto et al. (2002) stated that the quadratic model is preferred for closed systems. A quadratic model expressing CO_2 and H_2O concentrations as a function of time since closing the system can be written as:

$$CO_2 = a + bt + ct^2 \qquad \text{[eq 1.5]}$$

$$H_2O = a + bt + ct^2 \qquad \text{[eq 1.6]}$$

$\delta CO_2/\delta t$ and $\delta H_2O/\delta t$ are obtained by differentiating these equations with respect to time (t):

$$\frac{\partial CO_2}{\partial t} = b + 2ct_0 \qquad \text{[eq 1.7]}$$

$$\frac{\partial H_2O}{\partial t} = b + 2ct_0 \qquad \text{[eq 1.8]}$$

where t_0 is the time when ambient conditions were predicted to occur within the chamber. The slope is computed by solving the first derivatives at the time = t_0.

While a quadratic model is generally the best choice compared to a linear model for calculating $\delta CO_2/\delta t$ and $\delta H_2O/\delta t$, situations exist where the flux calculated using this model might be incorrect. For this study, a quantitative method for discriminating

between regression models was developed. A program was written (MATLAB, The Mathworks Inc., Natick, MA) to quantitatively decide between a linear or quadratic model. Because the quadratic model is highly prevalent in the literature, the program initially accepted all quadratic models. The quadratic models were then tested using three criteria. First, the shape of the quadratic curve was tested. Specifically, the program determined if the quadratic model predicted a local minimum or maximum value within the 40-s sampling period (Fig. 1.7). Also, the derivatives at 30s and 60s were compared (Fig. 1.8). If the minimum or maximum CO_2 or water vapor concentration; respectively, was observed within the 40-s time period, or if the derivative at 30-s was less than the derivative at 60-s, a linear model flux was utilized. Quadratic models that predicted a minimum or maximum value during sampling were discarded as the minimum and maximum values of CO_2 and water vapor, respectively, would be expected to occur at the end of the reading. The final check was testing if the quadratic model predicted that ambient conditions were achieved inside the chamber within the range of 15 s of placing the chamber on the soil frame. The time that conditions within the chamber matched ambient conditions was used for t_0 in predicting $\delta CO_2/\delta t$ and $\delta H_2O/\delta t$. If the predicted time that conditions within the chamber matched ambient conditions was outside this time frame, a linear model was utilized. Using these three criteria, the quadratic flux estimate was utilized for 80.1% of all NCE flux calculations, 14.2% of the ecosystem respiration flux calculations, and 99.5% of water vapor flux calculations (Table 1.1).

Comparison of Chamber and Eddy Correlation Fluxes

The definitive confirmation of the gas exchange chamber was the comparison of carbon fluxes measured with the clear chamber to other common methods of flux measurements specifically eddy correlation. The comparisons were conducted in an ungrazed, annually burned, native tallgrass prairie. While soil types differed between the sites, similar vegetation dominated each site. The chamber readings were conducted over a 40 s sampling interval, while the eddy correlation values are 30 min averages. Overall, seasonal trends of NCE measured by both methods were similar (Fig. 1.9 a,b). Differences between the two methods are probably due to soil types, size of sample area, and length of measurement.

Conclusion

The non-steady-state chamber described in this chapter couples a novel chamber design with precision instruments capable of fast sampling rates that in combination minimize microclimate disturbance. Throughout the two-year study, average chamber temperature increased 2.88° C, while chamber pressure increased only 0.32-Pa during measurements, and PAR attenuation was approximately 10%. One key component of minimizing microclimate changes during a sampling period was to perform rapid measurements. The current configuration samples considerably faster than many other chambers, which remain on plots for as long as 3 minutes (Wagner and Reicosky 1992, Pickering et al. 1993. Wilsey et al. 2002). Also, a logical framework for determining the correct regression model also was developed. The method allowed for a non-biased decision regarding the appropriateness of the quadratic model based on a series of predefined criteria.

References

Angell, R. and T. Svejcar. 1999. A chamber design for measuring net CO_2 exchange on rangeland. Journal of Range Management 52:27-31.

Bernacchi C.J., A.R. Portis, H. Nakano, S. von Caemmerer, and S.P. Long. 2002. Temperature response of mesophyll conductance. Implications for the determination of Rubisco enzyme kinetics and for limitations to photosynthesis in vivo. Plant Physiology 130:1992–1998.

Bremer, D.J. and J.M. Ham. 2005. Measurement and partitioning of in situ carbon dioxide fluxes in turfgrasses using a pressurized chamber. Agronomy Journal 97:627-632.

Ham, J., J. Murphy, and C.E. Owensby. 2005. Research Note: Measurement of net CO_2 exchange from tallgrass prairie using a nonsteady-state clear chamber. Kansas State University Internal Review.

Ham, J. 2006. Research Note: Vent tube design for whole-canopy flux chambers. Kansas State University Internal Review.

Hunt, S. 2003. Measurements of photosynthesis and respiration in plants. Physiologia Plantarum 117: 314–325.

Lund, C.P., W.J. Riley, L.L. Pierce, and C.B. Field. 1999. The effects of chamber pressurization on soil-surface CO_2 flux and the implications for NEE measurements under elevated CO_2. Global Change Biology 5:269–281.

Owensby, C.E., J.M. Ham, A.K. Knapp, D.J. Bremer, and L.M. Auen. 1997. Water vapour fluxes and their impact under elevated CO_2. Global Change Biology 3:189–195.

Pickering, N.B., J.W. Jones, and K.J. Boote. 1993. Evaluation of the portable chamber technique for measuring canopy gas-exchange by crops. Agriculture and Forest Meteorology 63:239–254.

Reicosky, D.C. and D.B. Peters. 1977. A portable chamber for rapid evapotranspiration measurements on field plots. Agronomy Journal 69:729-732.

Risch, A.C. and D.A. Frank. 2006. Carbon dioxide fluxes in a spatially and temporally heterogeneous temperate grassland. Oecologia 147: 291–302.

Steduto, P., O. Cetinkoku, R. Albrizio, and R. Kanber. 2002. Automated closed system chamber for continuous field crop monitoring of CO_2 and H_2O fluxes. Agriculture and Forest Meteorology 111:171-186.

Wagner, S.W. and D.C. Reicosky. 1992. Closed chamber effects on leaf temperature, canopy photosynthesis, and evapotranspiration. Agronomy Journal 84:731-738.

Wagner, S.W., D.C. Reicosky, and R.S. Alessi. 1997. Regression models for calculating gas fluxes measured with a closed chamber. Agronomy Journal 89:279-284.

Williams, R.E., B.W. Allred, R.M. Denio, and H.E. Paulsen, Jr. 1968. Conservation, development and use of the world's rangelands. Journal of Range Management 21:355-360.

Wilsey B.J., G. Parent, N.T. Roulet, T.R. Moore, and C. Potvin. 2002. Tropical pasture carbon cycling: relationships between C source/sink, above-ground biomass and grazing. Ecology Letters 5:367–376.

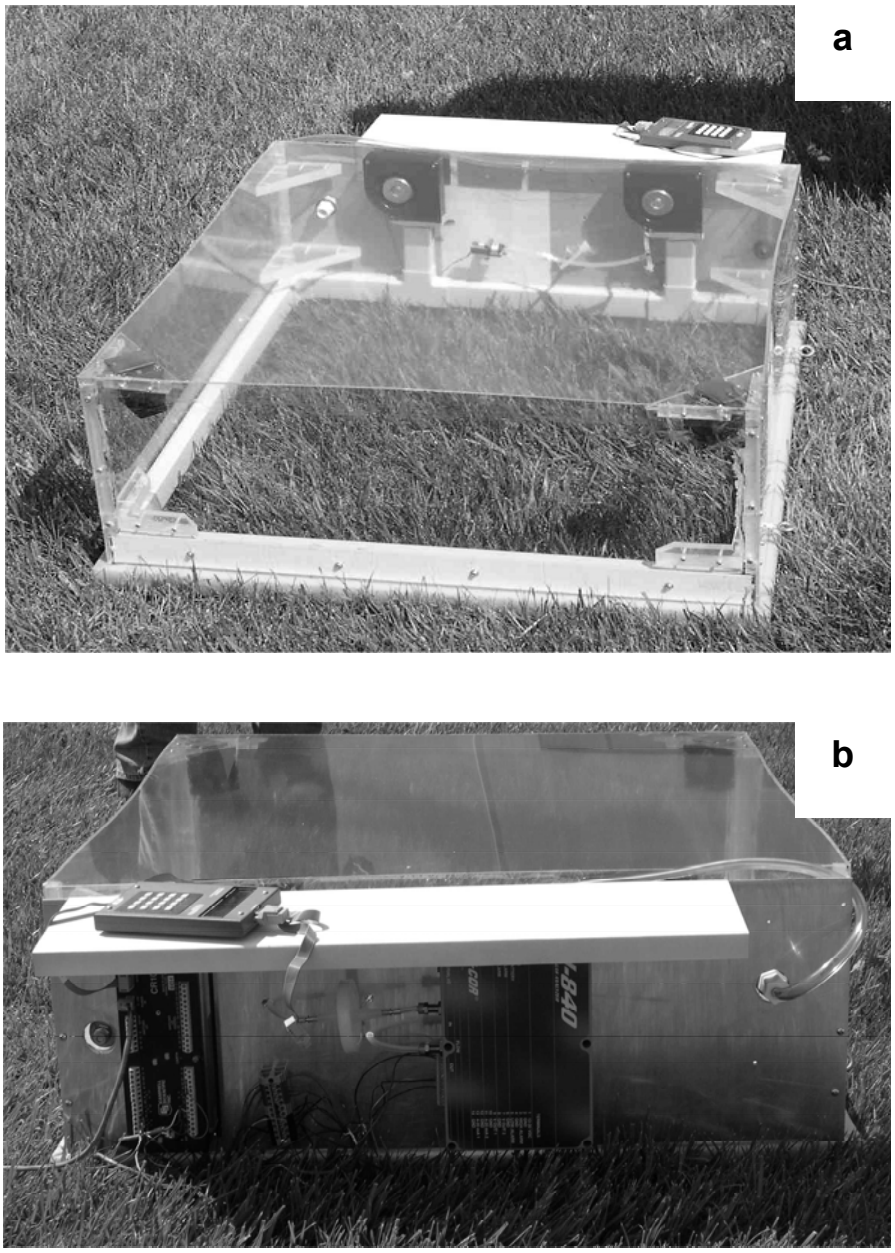

Figure 1.1. Picture taken of the chamber from opposite the IRGA (a). The light colored raceway along chamber bottom is air plenum. The foam strip along bottom seals the chamber to the soil frame. Picture taken from IRGA side of chamber showing the IRGA and the CR10X (b).

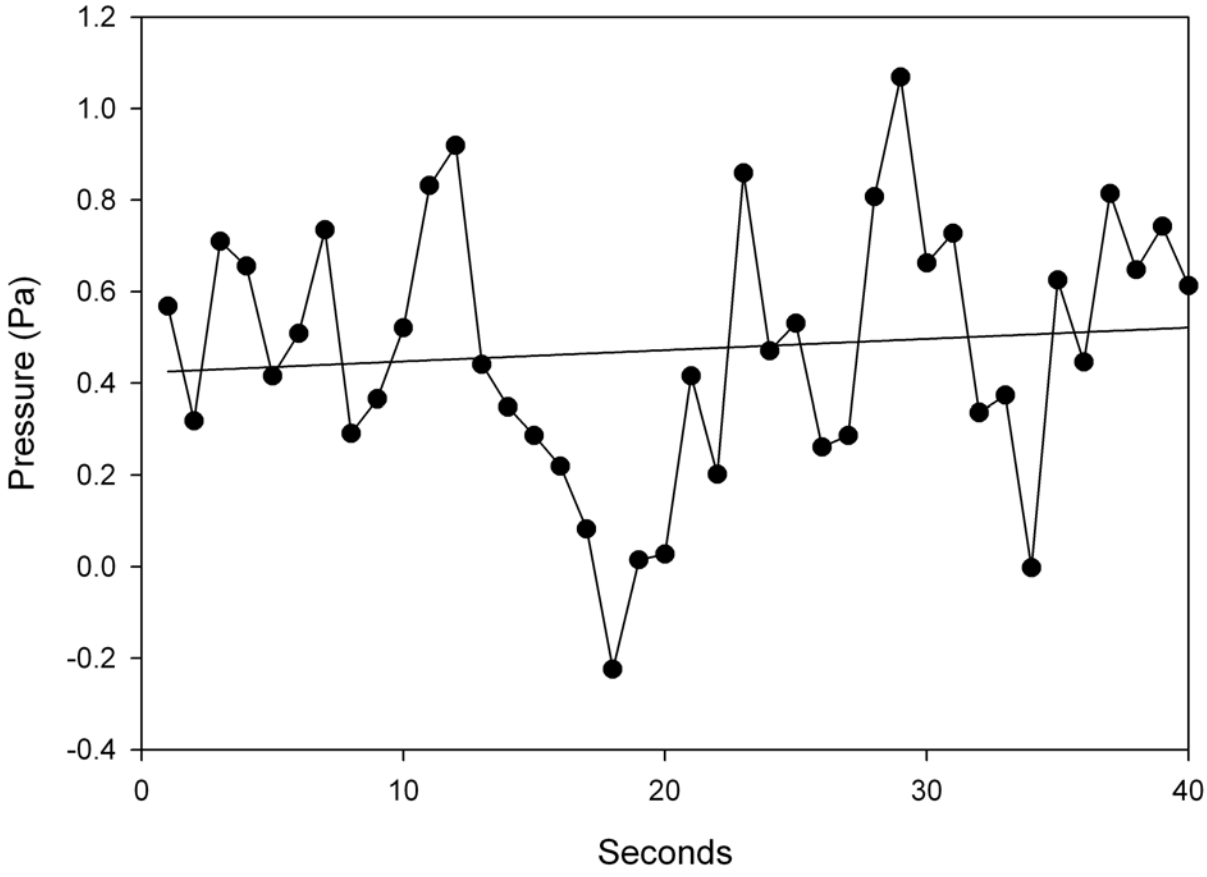

Figure 1.2. A typical example of chamber pressure observed during the 40 s measurement in the field. The solid black line represents the linear regression equation ($y = 0.0025x + 0.4226$ $r^2 = 0.01$).

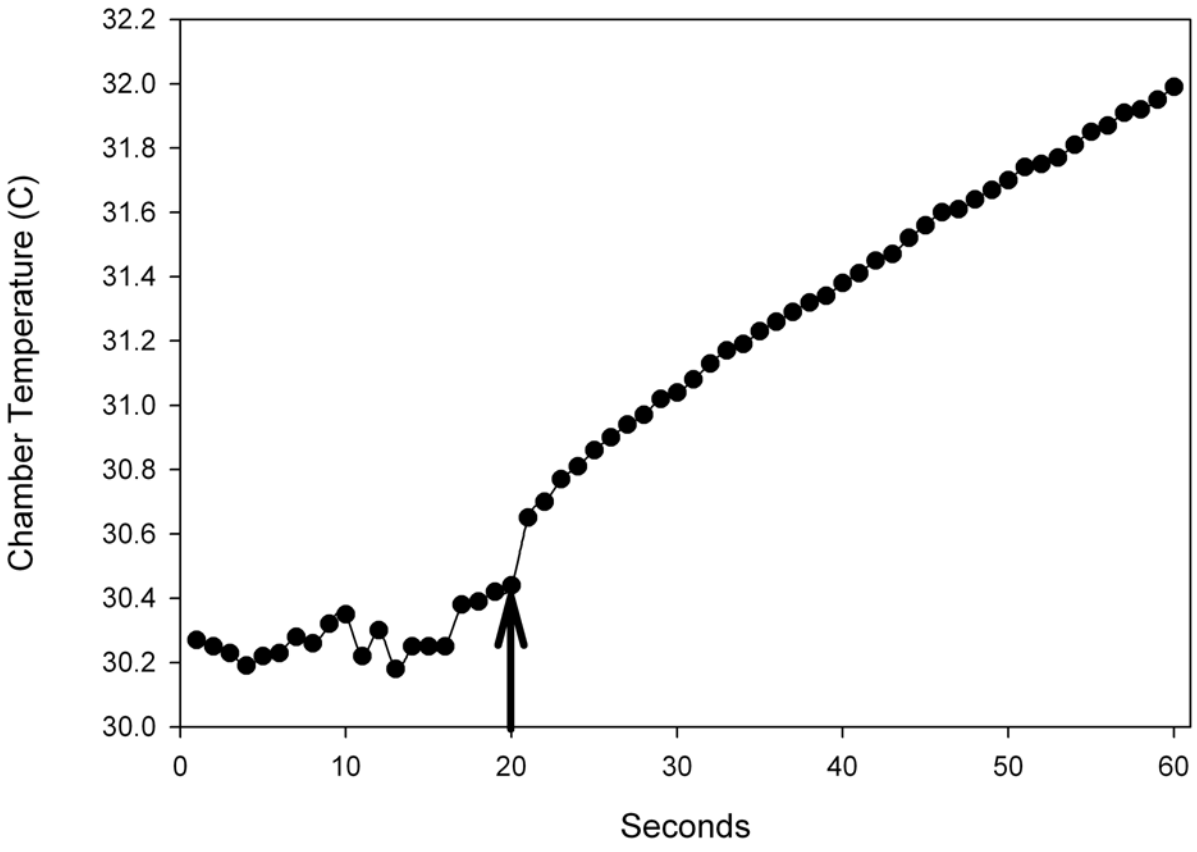

Figure 1.3. Typical air temperature inside the clear chamber observed during measurements in the field. The solid black arrow at 20 seconds indicates lowering of the chamber over the grass canopy.

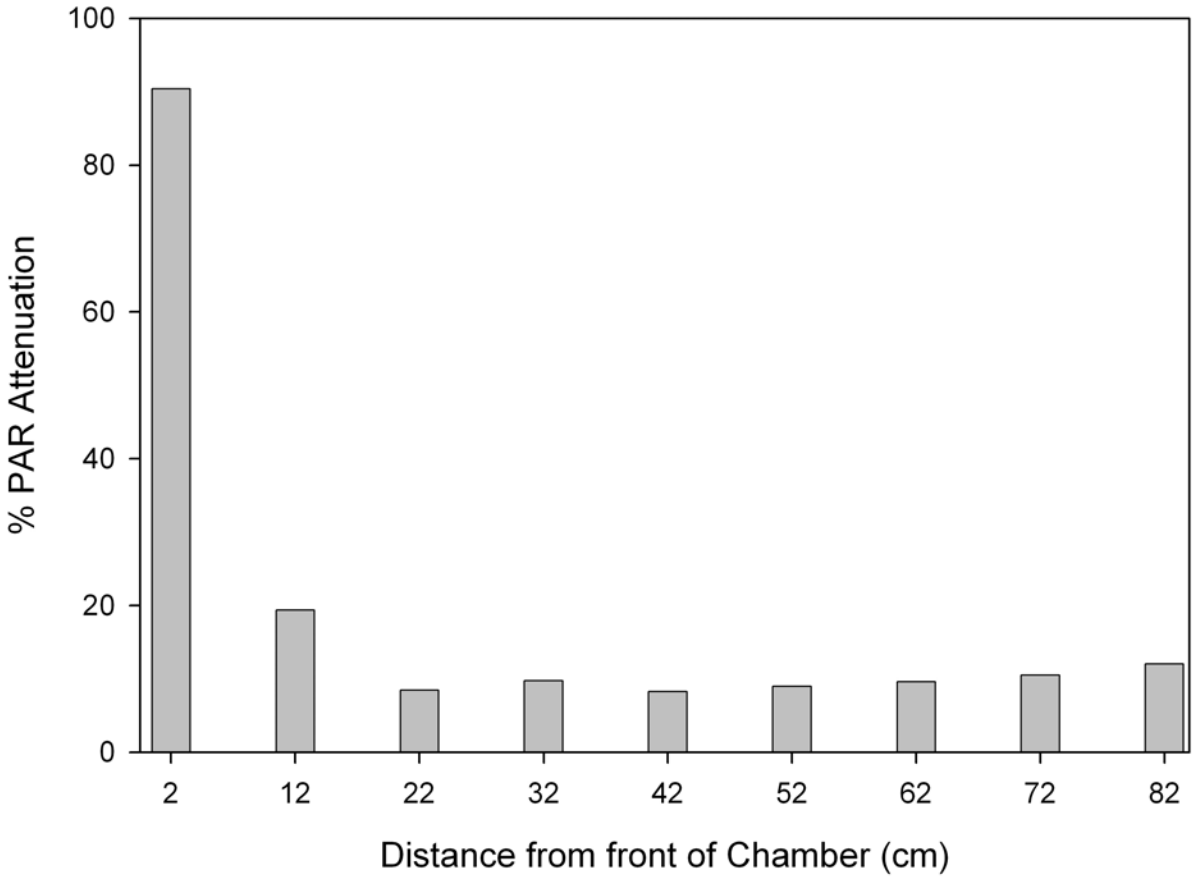

Figure 1.4. Percent of photosynthetically active radiation (PAR) attenuated by the clear chamber construction materials. Measurements of PAR attenuation began 20-mm from the side of the chamber opposite the IRGA with subsequent measurements taken every 100-mm.

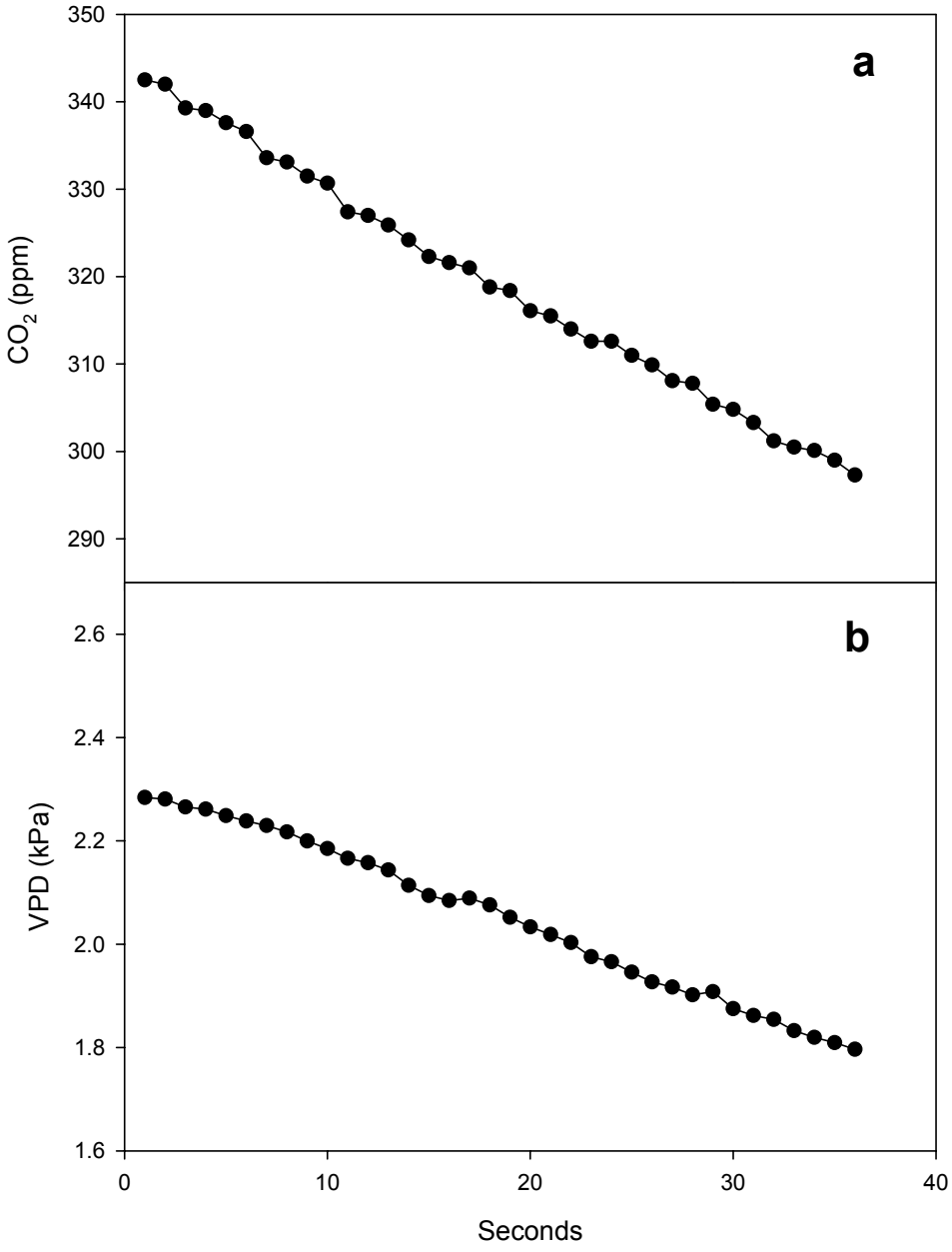

Figure 1.5. The rate change of CO_2 (a) and VPD rise (b) measured by a clear chamber over a well watered, full grass canopy.

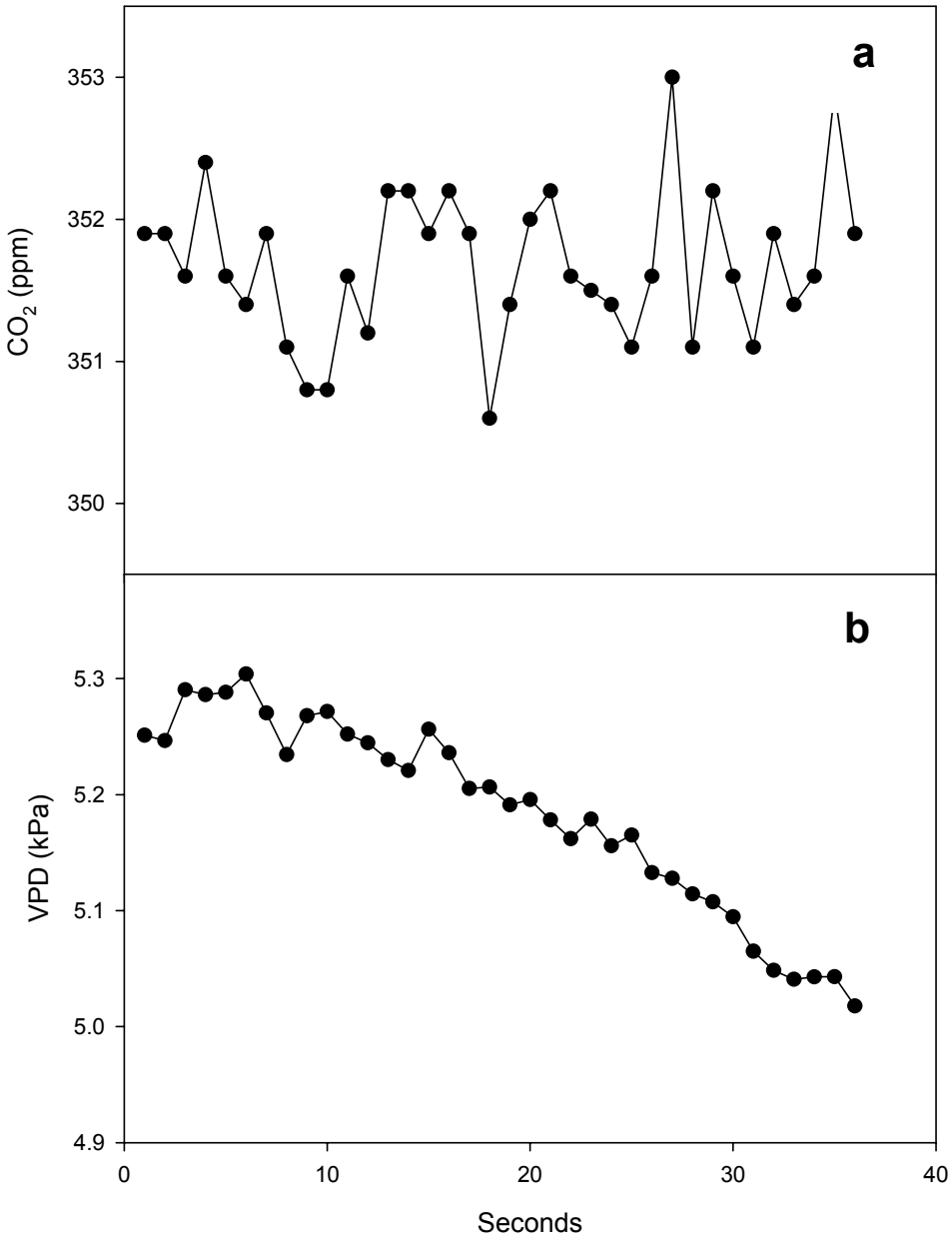

Figure 1.6. The rate change of CO_2 (a) and VPD rise (b) measured by a clear chamber on a plot with the leaf area recently removed by clipping all vegetation to a height of 5 cm.

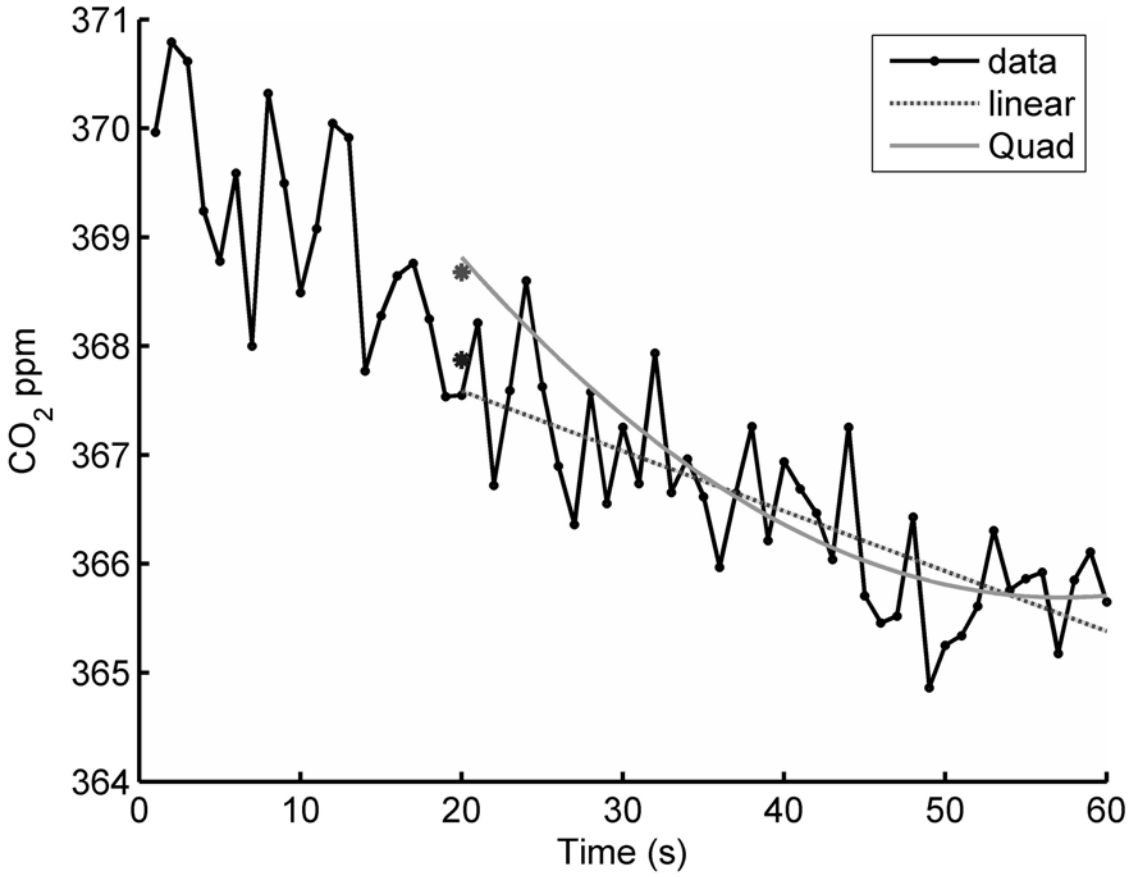

Figure 1.7. Actual CO_2 concentration recorded by the IRGA (data) and rate of change of CO_2 as calculated by the linear and quadratic (quad) models. The quadratic model predicted that the minimum value should occur at 50 s so a linear model was utilized in calculating the flux.

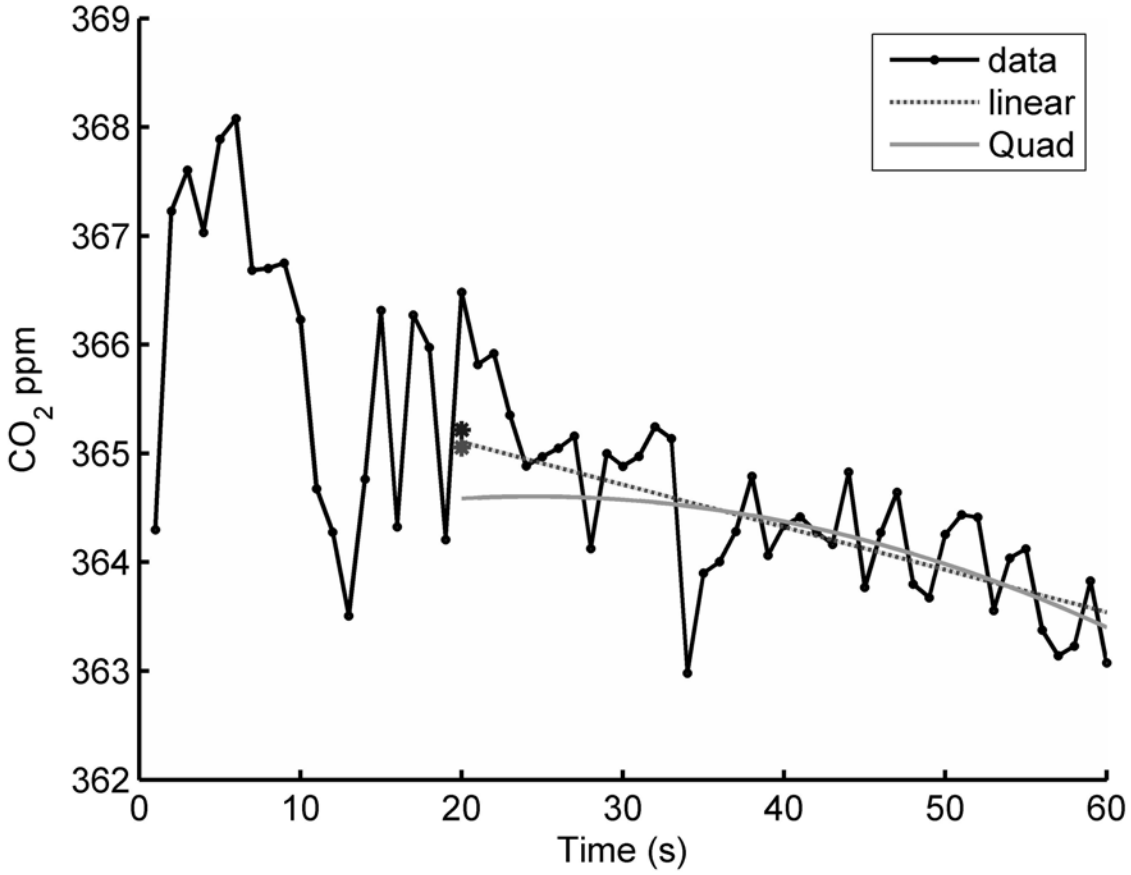

Figure 1.8. Actual CO_2 concentration recorded by IRGA (data) and rate of change of CO_2 as calculated by the linear and quadratic (quad) models. The quadratic model predicted that the slope of the quadratic model was less at 30 s than at 60 s therefore a linear model was used to calculate the flux.

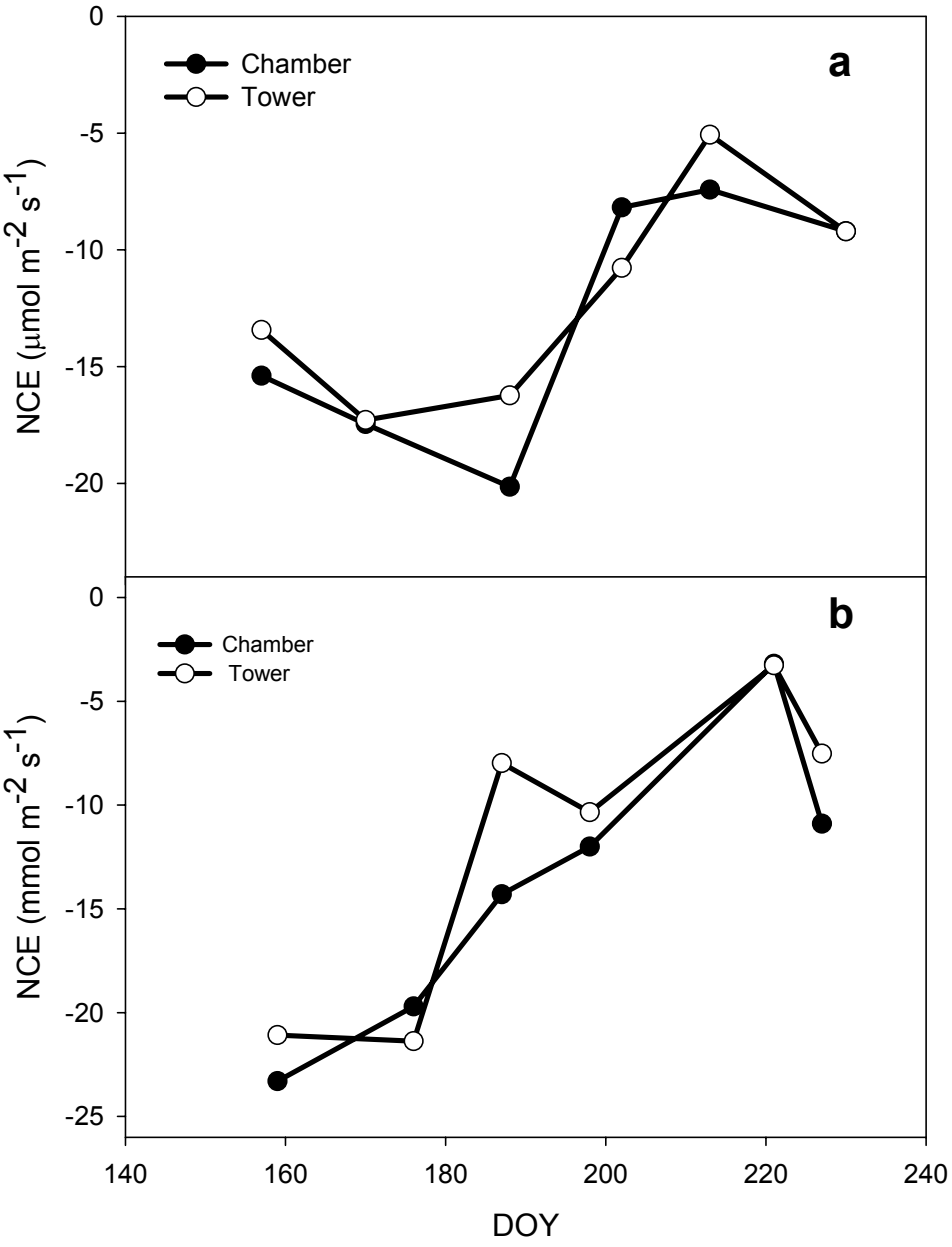

Figure 1.9. Net Carbon Exchange (NCE) of a tallgrass prairie measured by a clear chamber and eddy correlation on six dates during 2005 (a) and 2006 (b).

Table 1.1 The percent of net carbon exchange, ecosystem respiration, and water vapor fluxes calculated with quadratic models that were rejected for each year of the study (2005, 2006) due to violations of the criteria for shape of the predicted curve (Shape) or outside of the time frame for conditions within the chamber to match ambient conditions (Range).

	Net Carbon Exchange		Ecosystem Respiration		Water Vapor	
Criteria	**2005**	**2006**	**2005**	**2006**	**2005**	**2006**
Shape	20.7%	16.5%	89.0%	82.3%	0.24%	0.63%
Range	2.4%	0.2%	0.0%	0.3%	0.24%	0.0%

CHAPTER 2 - Patterns of CO_2 and Water Vapor Flux Following Harvest of Tallgrass Prairie at Different Times

Abstract

Rangelands occupy 47% of the ice-free terrestrial landmass. Virtually all rangelands are harvested at some point during the year. While the immediate effect of harvesting is the removal of plant leaf area and biomass, it also alters a host of ecosystem processes. An experiment was conducted from June-October of 2005 and 2006 to determine the effect of clipping date on subsequent CO_2 and water vapor fluxes of a tallgrass prairie. Eighteen, 0.85 m x 0.85 m plots were established during mid-May both years. Every two weeks, all vegetation within three different plots was clipped to a height of 5 cm. Using a transparent gas exchange chamber, CO_2 and water vapor fluxes were measured on 12 different dates from the beginning of June through mid-October. The immediate effect of all clipping treatments was a loss of leaf area and reductions in gross canopy photosynthesis (GCP), net carbon exchange (NCE), and ecosystem respiration (R_E) and, in most cases, a decreased water vapor flux. Periods of drought during both seasons also decreased GCP, NCE, R_E, and water vapor flux. However, following subsequent late season rainfall, patterns of carbon flux appear to be governed by the amount of water stress during canopy development. Canopies that developed during periods of low water stress quickly increased carbon fluxes when water availability increased. However, fluxes from canopies that developed under water stress, responded considerably slower to subsequent increases in water availability.

While carbon fluxes appear to be influenced by water stress during canopy development, water vapor fluxes were most closely associated with soil water content.

Introduction

Rangelands are one of the most common ecosystems worldwide covering approximately 47% of the terrestrial landmass (Williams et al. 1968). Virtually all rangelands are grazed by livestock or native grazers at some point during the year. While the immediate effect of grazing is the removal of plant leaf area and biomass, grazing also alters a host of ecosystem processes (Bremer et al. 1998, 2001, Craine et al. 1999, Owensby et al. 2006).

The removal of upper leaves allows light to penetrate deeper into the canopy (Gold and Caldwell 1990). Because meristematic tissue is typically located below ungulate grazing height, a canopy of younger leaves is also a product of grazing. Gold and Caldwell (1990) reported that the increased light penetration and greater proportion of younger leaves led to increased photosynthetic rates per unit leaf area. Similarly, Wallace (1990) reported that regrowth from grazed plants has greater photosynthetic rates than leaves of ungrazed plants.

However, removal of more than 50% of the leaf area of grass stops root growth for up to 6 weeks (Crider 1955) and limits nitrogen uptake. Excessive loss of photosynthetic tissue, forces plants to rely on reserves of non-structural carbohydrates (TNC) and nitrogen for regrowth. Range plants demonstrate cycling of both TNC and nitrogen (McKendrick et al. 1975, Owensby et al. 1977). These cycles result in low concentration of TNC and nitrogen in rhizomes, crowns, and stem bases during periods of active growth when plant requirements exceed either photosynthesis or nitrogen uptake.

Following defoliation, Davidson and Milthorpe (1966) and Gonzalez et al. (1989) reported decreasing reserves of carbon in storage organs. Using carbon isotope tracers, de Visser et al. (1997) confirmed that the pre-defoliation carbon in storage organs was being utilized in regrowth for two days following clipping and was responsible for 50% of total carbon used in regrowth three days post clipping. Richards and Caldwell (1985) reported that carbon reserves were important contributors to regrowth for 2.5 days following severe defoliation of the bunchgrasses *Agropyron desertorum* (Fisch. Ex Link) Schult. and *A. spicatum* (Pursch) Scribn. & Smith.

The amount of TNC reserves also impacts photosynthetic rates of regrowth. Working in a well-watered, fertilized environment, Danckwerts (1993) reported that net photosynthetic rates of kangaroo grass (*Themeda triandra* Forsk.) were higher when plants had greater carbon reserves. These results demonstrate the potential importance of the level of TNC reserves at the time of clipping.

Nitrogen reserves are also important for regrowth following grazing. Nitrogen deficiencies may lead to decreased chlorophyll and ribulose-1-5-bisphosphate carboxylase (Rubisco) production (Coyne et al. 1995). Ourry et al. (1988) reported that nearly all nitrogen for new leaf growth for perennial ryegrass was derived from internal reserves for six days following clipping. During the same time, they also reported that uptake of nitrogen from the soil was very low. These results confirmed those reported by Clement et al. (1978), who reported a decline in uptake of NO_3^- for seven days and that the rate of uptake did not recover until a positive carbon balance by the plant was achieved. These results suggest that nitrogen reserves are important at time of leaf removal.

Craine et al. (1999) concluded that factors that affect carbon availability to roots also affect soil CO_2 flux. While grazing increases photosynthesis on a per unit leaf area basis, it reduces photosynthate allocated to the roots. The result is a reduction in soil CO_2 flux. Bremer et al. (1998) reported that grazing reduced daily soil CO_2 flux by 20-37%, as compared to ungrazed pastures.

Bremer et al. (2001) constructed a conceptual model on the impact of grazing on the partitioning of energy between the canopy and soil surface. Following removal of leaf area by grazing, more irradiance penetrates the canopy and reaches the soil surface, resulting in increased evaporation from the soil surface and decreased transpiration. The alteration of energy partitioning decreased daily evapotranspiration (ET) up to 40% and reduced seasonal ET by 6.1% (Bremer et al. 2001). The reductions in ET led to increased amounts of soil moisture in the top 30 cm of the soil. This further substantiated work of Owensby et al. (1970) that reported increased soil water when grass was clipped. Increased soil temperatures and conserved moisture in the top 30 cm may, however, act to increase microbial respiration in grazed pastures. The conserved soil moisture may also moderate seasonal droughts allowing grazed pastures to maintain greater photosynthetic rates due to increased water availability.

Inter-annual precipitation variability also affects productivity of grasslands (Knapp and Smith 2001). Productivity of burned tallgrass prairie is significantly related to precipitation (Briggs and Knapp 1995). Furthermore, a synthesis of net ecosystem exchange (NEE) measurements by eddy covariance demonstrated positive NEE values (source of CO_2) occurred with drought during the growing season (Novick et al. 2004).

These factors interact to produce varying results at the landscape level. Working in the tallgrass prairie of Kansas, Owensby et al. (2006) reported that grazed and ungrazed systems had similar cumulative CO_2 fluxes. They attributed this to increased photosynthetic efficiency and decreased respiration in grazed pastures. Morris and Jensen (1998), working in a Denmark saltmarsh, reported increased weight specific rates of gross photosynthesis and reduced canopy respiration rates at a grazed site. However, soil respiration rates between grazed and ungrazed marshes were similar. This resulted in no detectable differences in net ecosystem productivity between the grazed and ungrazed marshes. Furthermore, Wilsey et al. (2002) reported decreased ecosystem respiration rates, but similar NEE when comparing grazed and ungrazed tropical pastures in Panama. Lecain et al. (2000) reported higher rates of NCE on grazed pastures compared to ungrazed pastures, but the response of soil respiration was variable in relationship to grazing.

Evaluating the effect of grazing on net carbon exchange is challenging because many factors other than biomass removal affect CO_2 fluxes. Grazing affects both canopy and soil fluxes, thus gas exchange must be studied using land area rather than at the leaf level alone. A central question is how does biomass removal interact with environmental factors (precipitation, temperature, etc.) and plant phenology to impact gas exchange over the growing season. The hypothesis of this study was that canopies clipped when reserves of non-structural carbohydrates and nitrogen were low would have lower rates of photosynthesis during the initial phase of regrowth. Murphy (2007) described a new whole-canopy chamber system that is well suited for measuring carbon fluxes from small rangeland plots arranged in a statistical design. Removing biomass

by clipping instead of by grazing is another way to create more statistical control of variables affecting gas exchange in a plot-scale study.

The objective of this study was to assess the impact of clipping date and natural growing season precipitation on gross canopy photosynthesis (GCP), net carbon exchange (NCE), ecosystem respiration (R_E), and water vapor (WVF) fluxes from a tallgrass prairie.

Materials and Methods

Study Area

The study was conducted from June through October during 2005 and 2006. The site was an ungrazed, annually burned pasture located in the Rannells Flint Hills Prairie Preserve, 5-km south of Manhattan, KS (39.11°N, 96.34°W, 324 m above sea level). The dominant vegetation consisted of the native C4 species *Andropogon gerardii* Vitman and *Sorghastrum nutans* (L.) Nash while subdominants included *A. scoparius* Michx. and *Bouteloua curtipendula* (Michx.) Kunth. The remainder of the vegetation consisted of various sedges (C3), and C3 forbs including *Vernonia baldwinii* (Small) Schub., *Ambrosia psilostachya* DC., *Artemesia ludoviciana* Nutt., and *Psorelea tenuiflora* var. *floribunda* (Nutt.) Rydb. The soil was a Dwight silty clay (Fine, smectitic, mesic Typic Natrustolls) on a 1-3% slope. Average annual precipitation (1971-2000) was 884 mm with 542 mm occurring from May through September. The majority of the Flint Hills is grazed by yearling steers stocked either from May through October (1.62 ha steer^{-1}) or intensive early stocking from May through mid-July (0.81 ha steer^{-1}) (Smith and Owensby 1978).

Experimental Design

Eighteen plots, 0.85 m x 0.85 m, were established in mid-May of 2005 and 2006. The plots were arranged in a randomized complete block design of three blocks with six treatments per block. The six treatments were randomly assigned to plots within a block. Because photosynthesis has a curvilinear response to increasing irradiation, the blocks were always sampled in the same order and the blocking factor was organized based on the order the plots were sampled.

The experimental treatment was day of year the plot was clipped. A treatment consisted of clipping all vegetation within the plot and a 50 cm buffer strip outside of the plot to a 5-cm height. The first treatments were scheduled for 5 June 2005 and 6 June 2006, respectively. Successive treatments were scheduled to begin 14-, 28-, 42-, 56-, and 70-days after the initial treatment. Variations in treatment start dates resulted from the necessity of making measurements on cloudless days. Only clipped, or plots scheduled to be clipped on that day, were included in those days' measurements.

Measurements of CO_2 and Water Vapor Fluxes

Net carbon exchange, R_E and water vapor fluxes were measured with non-steady-state closed system chamber (Chap. 1). The chamber area was 0.85-m x 0.85-m with a height of 0.25-m and total weight of 10.9 kg. Sides were constructed of 4.59-mm acrylic-FE (Acrylite, Cyro Industries, Clifton, NJ). The top was made from heat-stretched Propafilm-C (ICI Americas Inc., Wilmington, DE) with high thermal and visible transmittance (Hunt 2003). A closed-cell foam gasket (nomapack-WS, Nomaco Inc, Zebulon, NC) provided a tight seal between the bottom edges of the chamber sides and the soil collar. Two fans (700 L min^{-1}, BD 12A3, Comair Rotron, San Diego, CA)

circulated air through a perforated plenum attached to the inside wall near the bottom of the chamber. The rate change of CO_2 concentration within the chamber was measured with a closed path infrared gas analyzer (IRGA, LI-840, Li-Cor Industries, Lincoln, NE). Net carbon exchange was measured with the chamber exposed to ambient light. All readings occurred between 1030-1500 (LST) during clear days. Readings were taken on 24 dates between June to September and June to October in 2005 and 2006. Chamber measurements were initiated by recording ambient conditions above the canopy for 20 seconds. Data acquisition was then paused for five seconds while the chamber was positioned over the canopy and placed onto the soil frame. The collars were 0.85 m x 0.85 m, constructed of 5.1 cm x 7.6 cm x 0.5 cm angle iron with the top of the frame extending 5 cm above the soil surface. Following the five-second pause, data acquisition resumed for a 40-second period with the chamber positioned over the canopy. Following each reading, the chamber was removed from the canopy and the CO_2 and water vapor concentrations and air temperature within the chamber were allowed to equilibrate with ambient conditions. Ecosystem respiration was then measured by excluding light with an opaque cover for the chamber and the opaque chamber positioned over the canopy. The sampling procedure was the same as NCE readings. Gross Canopy Photosynthesis (GCP) is:

$$GCP = NCE + R_E \qquad \text{[eq 2.1]}$$

all expressed in μmol m^{-2} s^{-1}. Since R_E in the dark is greater than in the light, because of increased canopy respiration, the calculated GCP was slightly overestimated (Brooks and Farquhar 1985, Wohlfahrt et al. 2005). Working with three *Poa* species, Atkin et al. (1997) reported that canopy respiration in the dark increases between 16 and 77%

compared to that in the light. However, in the tallgrass prairie, soil respiration is typically much larger than canopy respiration because a large portion of the biomass is belowground. Soil respiration is between 75% and 100% of R_E depending on the size of the canopy (Bremer and Ham 2002). Assuming canopy respiration in the opaque chamber increased by 35% over canopy respiration in the light and that canopy respiration was 20% of R_E, a recalculation showed that overestimates of 2006 GCP were probably around 3%. The micrometeorological convention of labeling fluxes from the ecosystem to the atmosphere as positive (source of CO_2) was utilized in this study.

Environmental Measurements

During each NCE reading, soil temperature, air temperature and photosynthetically active radiation (PAR) were measured simultaneously. Soil temperature was measured with a thermocouple (Type T, 0.5 mm diameter) epoxied in a hypodermic needle (1.7 mm O.D. diameter) and inserted into the buffer strip to a 5 cm depth. Air temperature was recorded within the chamber with an aspirated 0.4-mm-diameter thermistor (10K3MCD1, Betatherm Corp., Shrewburg, MA). A quantum sensor (LI-190, Li-Cor Industries) measured PAR above the chamber. Soil moisture in the top 20 cm of the clipped buffer strip outside of the soil frame was measured gravimetrically with the dry weight determined by drying one sample from each plot for 48 hrs at 105°C.

Statistical Analysis

The effect of clipping date on NCE, R_E, GCP, and water vapor fluxes and all ancillary environmental measures were analyzed separately for each year using a

mixed analysis of variance model where treatment was the fixed effect and block was the random effect (PROC MIXED SAS 9.1, SAS Institute, Cary, NC). Mean flux values were compared using least-square means analysis (PROC LSMEANS, SAS 9.1) with significance determined at the $p < 0.05$ level.

Results

Environmental Conditions

2005.

Average monthly air temperatures measured in Manhattan, KS were near the 30-yr averages (Fig. 2.1). While total precipitation was near average, timing of precipitation deviated from the 30-year average. Precipitation received from May-September was 102 mm above the average. However, precipitation during May and July was only 29% and 55% of the average, respectively. June precipitation was more than double the average with 288 mm (96%) received during the first 11 days of the month.

2006.

Similar to 2005, average monthly air temperatures were near the 30-year average; however, total precipitation was 13% below the average (Fig. 2.1). The amount of precipitation received from May-September was near normal, but May and June precipitation was well below normal and August precipitation was nearly three times the long-term average. The majority (63%) of the August precipitation was received during a 10-day span in the middle of the month.

Soil Temperature

2005.

Soil temperatures were not different among treatments for any sampling date during 2005. Soil temperatures increased from the initial treatment on DOY 157 reaching a maximum temperature on DOY 220 (Fig. 2.2a). Soil temperatures then gradually declined through the end of the growing season with the minimum temperature recorded on DOY 259.

2006.

Soil temperatures in 2006 followed a similar pattern to 2005 soil temperatures. Temperatures increased from the initial treatment on DOY 160 until the maximum temperature was recorded on DOY 221 (Fig. 2.2b). Soil temperatures then declined throughout the rest of the growing season with minimum temperatures recorded on DOY 285. However, unlike 2005, treatments affected soil temperature on three occasions in 2006: DOYs 177, 243, and 256. On DOY 177, soil temperatures from plots clipped on DOY 160 were significantly higher ($p = 0.04$) than pre-clipped temperatures for plots clipped on DOY 177. On DOY 243, soil temperatures of plots clipped on DOY 160 were significantly ($p = 0.01$) less than all plots except those clipped on DOY 221. On DOY 256, temperatures of plots clipped on DOY 160 were significantly ($p = 0.009$) less than all other plots.

Soil Water Content

2005 and 2006.

Soil water content in the top 20 cm was not significantly different among treatments on any sampling date. Soil water content varied according to rainfall events. During 2005, maximum soil water content was measured early in June and decreased until mid to late August (Fig. 2.3a). Soil water content during 2006 was lower in the early growing season, with the greatest water content measured during mid September (Fig. 2.3b).

2005 Flux Rates

Gross Canopy Photosynthesis Fluxes (GCP).

Approximately 5-10 days after clipping, GCP was lower than pre-clip levels for all plots (Figs 2.4a, b, c). Gross canopy photosynthesis flux rates from plots clipped on DOY 157 and DOY 170 quickly increased and were similar to pre-clip rates on DOY 188. Fluxes from these plots increased for 30 and 25 days, respectively, until apparent moisture stress caused the rates to decline. However, following late season precipitation (Fig. 2.1b), GCP from the plots quickly increased until DOY 242. By the end of the season, DOY 259, GCP rates declined as the canopies began senescing.

Gross canopy photosynthesis fluxes from plots clipped on DOYs 188, 202, and 213, during the mid-summer drought, showed little increase in flux rates for up to 25 days following clipping. Even following late season precipitation, GCP from plots clipped during the mid-season drought were significantly lower ($p = 0.0002$) than plots clipped on DOY 157 and DOY 170. However, GCP from plots clipped later in the

season continued to increase through the final reading of the season on DOY 259 and were similar to plots clipped on DOY 157 and DOY 170 ($p = 0.16$).

Ecosystem Respiration flux rates (R_E).

Similar to GCP, R_E, for approximately 5-10 days following clipping, was lower than pre-clip levels for all plots (Fig 2.5a, b, c). However, fluxes from plots clipped on DOY 157 and DOY 170 did not show the same pattern of recovery as GCP did from the same plots. Ecosystem respiration fluxes from plots clipped on DOY 157 slightly increased for 20 days following clipping, while R_E from plots clipped on DOY 170 remained relatively constant. However, R_E from both sets of plots began declining as soil water became limiting. Similar to GCP, following late season precipitation (Fig. 2.1b), R_E quickly increased until DOY 242. By the last measurement of the season, DOY 259, fluxes declined.

Ecosystem respiration fluxes for plots clipped on DOY 188, DOY 202, and DOY 213, during the mid-summer drought, declined following clipping. However, following the late season precipitation, R_E from these plots increased as quickly as did rates from plots clipped on DOY 157 and DOY 170. While GCP from plots clipped late in the season increased through the final measurement of the year, R_E from all plots declined on DOY 259.

Net Carbon Exchange Flux Rates (NCE).

Net carbon exchange fluxes from 2005 followed similar patterns to GCP from the same year. Approximately 5-10 days after clipping, NCE was lower than pre-clip levels for all plots (Figs 2.6a, b, c). Net carbon exchange fluxes from plots clipped on DOY 157 and DOY 170 quickly increased and were similar and slightly less, respectively,

than pre-clip rates on DOY 188. Fluxes from these plots increased for 30 and 25 days, respectively, until apparent moisture stress caused the fluxes to decline. However, following late season precipitation (Fig. 2.1b), NCE from the plots quickly increased until DOY 242. By the end of the season, DOY 259, NCE declined as the canopies began senescing.

Net carbon exchange fluxes from plots clipped on DOYs 188, 202, and 213, during the mid-summer drought, showed little increase in fluxes for up to 25 days following clipping. Unlike plots clipped on DOY 157 and DOY 170, each of these plots had positive NCE within 7-11 days following clipping. Even following late season precipitation, NCE from plots clipped on DOY 230 had positive flux rates following clipping. Again similar to GCP, NCE from plots clipped later in the season continued to increase through the final reading of the season on DOY 259 and were similar to plots clipped on DOY 157 and DOY 170.

Water Vapor Fluxes (WVF).

Similar to 2005 GCP, approximately 5-10 days after clipping WVF were lower than pre-clip levels for all plots except those plots clipped on DOY 230 (Fig. 2.7a, b, c). Water vapor fluxes from plots clipped on DOY 157 and DOY 170 quickly increased for 20 days, until apparent moisture stress caused rates to decline. Similar to 2005 GCP, WVF from the plots quickly increased until DOY 242. Though, unlike GCP from the same plots, WVF from these plots did not increase more quickly than any other plots following the precipitation events. By the end of the season, DOY 259, WVF declined as canopies senesced.

Water vapor fluxes from plots clipped on DOY 188 and DOY 202, during the mid-summer drought, increased only slightly for up to 15 days following clipping. However, following the late season precipitation (Fig. 2.1b), WVF from the plots matched the WVF from plots clipped on DOY 157 and DOY 170. Even though plots clipped on DOY 220 were also clipped during the mid-summer drought, levels increased as quickly as plots clipped on DOY 157 and 170. Water vapor fluxes from plots clipped on DOY 213 were not lower than pre-clip levels 12 days following clipping. Unlike 2005 GCP though, WVF declined for the final reading of the season on DOY 259.

2006 Flux Rates

Gross Canopy Photosynthesis Flux Rates (GCP).

Gross canopy photosynthesis fluxes were lower than pre-clip levels for all plots up to 23 days after clipping (Fig. 2.8a, b, c). Fluxes from plots clipped on DOY 160 increased for 30 days, while plots clipped on DOY 177 increased for only 7 days before apparent water stress caused rates to decline. Similar to GCP in 2005, following late season precipitation (Fig. 2.1b), GCP from the plots increased quickly until DOY 256. The GCP from these plots were similar to pre-clip GCP from plots clipped on DOY 227, and significantly greater than all other plots ($p < 0.0001$). On DOY 285, the end of the season, GCP declined as canopies began senescing.

Gross canopy photosynthesis fluxes from plots clipped on DOY 187, during the mid-summer drought, showed little increase in fluxes for 24 days following clipping. Similar to plots clipping during the 2005 mid-summer drought, GCP from these plots following late season rain were significantly lower ($p < 0.0001$) than plots clipped on

DOY 160 and DOY 177 until DOY 243. From DOY 256 through the end of the season, DOY 285, GCP declined and was similar to all other plots.

Gross canopy photosynthesis fluxes from plots clipped on DOYs 198, 221, and 227, just prior to and after the late season precipitation, respectively, quickly increased. By DOY 243, GCP from plots clipped on DOY 198 were similar to GCP from plots clipped on DOYs 160 and 177 and continued to increase until DOY 256. On DOY 256, GCP from plots clipped on DOYs 221 and 227 were similar to GCP from all other plots. GCP from these plots then decreased through the remainder of the growing season and were similar to GCP from all other plots.

Ecosystem Respiration fluxes (R_E).

Similar to 2005, R_E following clipping R_E from all plots, except those clipped on DOY 221, were lower than pre-clip levels for up to 23 days following clipping (Fig. 2.9a, b, c). Following clipping, R_E from plots clipped on DOY 160 increased gradually for 34 days, while R_E from plots clipped on DOY 177 increased only slightly for 17 days. Ecosystem respiration fluxes from these plots and plots clipped on DOY 187 then began declining as soil water content decreased. Ecosystem respiration fluxes from plots clipped just prior to the late season precipitation were lower than pre-clip levels, however, then quickly increased following the precipitation. These plots responded similarly to 2005 R_E to late season precipitation by quickly increase R_E. Following the precipitation, R_E increased for approximately 16-29 days before declining through the final measurement of the season on DOY 285.

Post-clip patterns of R_E from plots clipped on DOYs 221 and 227, which were clipped just prior to and after the late season precipitation, were different from all other

plots. Ecosystem respiration flux rates were higher than pre-clip rates six days following clipping and continued to increase for 29 days. Ecosystem respiration flux rates from plots clipped on DOY 227 remained relatively constant for 13 days. Both sets of plots then gradually declined in a similar manner to all other plots until the final reading of the season.

Net Carbon Exchange Fluxes (NCE).

Similar to 2005 NCE, 2006 NCE followed similar patterns to the current year GCP. Up to 23 days after clipping, NCE was lower than pre-clip levels (Fig. 2.10a, b, c). Net carbon exchange fluxes from plots clipped on DOY 160 and 177 quickly increased for 22 and 7 days, but were less than pre-clip levels from plots clipped on DOY 187. As soil moisture became limiting, the fluxes began declining. However, similar to GCP, following late-season precipitation, NCE from both sets of plots increased for 29 days and were similar to pre-clip levels from plots clipped on DOY 227 and were greater than the other plots. As the canopies began senescing, NCE declined through the end of the season and were similar to NCE from all other plots.

Net carbon exchange fluxes from plots clipped on DOYs 187 and 198, during the mid-summer drought, remained relatively unchanged up to 33 days after clipping. Even following the precipitation, NCE remained mostly unchanged. However, 16 days later, NCE from plots clipped on DOY 198 were similar to pre-clip levels from plots clipped on DOY 198. Nineteen days later, NCE from plots clipped on DOY 187 were similar to all other plots. Net carbon exchange fluxes continued to increase until DOY 256, before declining at rates similar to all other plots through the end of the season.

Plots clipped on DOYs 221 and 227 were clipped just prior to and after, respectively, the late season precipitation. Unlike any other plots from 2006, plots clipped on DOY 221 had positive NCE six days following clipping. However, NCE quickly increased and were similar to all other plots 29 days later. Net carbon exchange fluxes from plots clipped on DOY 227 increased for 13 days and were similar to all other plots on DOY 256 before declining at similar rates to all other plots.

Water Vapor Fluxes (WVF).

Clipping reduced WVF only from plots clipped on DOY 160, DOY 165, and DOY 198 (Fig. 2.11a, b, c). Water vapor fluxes from plots clipped on DOY 187, DOY 221, and DOY 227 remained similar or slightly increased compared to pre-clip levels. Water vapor fluxes from plots clipped on DOY 160 and 177 increased for 29 and seven days, respectively. Low water availability then caused WVF to decline. Following late season precipitation (Fig. 2.1b), WVF increased from the plots. However, unlike 2006 GCP, WVF from plots clipped on DOY 160 and DOY 177 increased at similar rates to all other plots. Water vapor fluxes began declining on DOY 268 as canopies began senescing.

Water vapor fluxes from plots clipped on DOY 187 remained almost unchanged following clipping and then declined slowly during the mid-summer drought. Following the late season precipitation, WVF from plots clipped on DOY 187 and DOY 198 increased quickly and were equal to or greater than WVF from plots clipped on DOY 160 and DOY 177 through the end of the season.

Plots clipped on DOY 221, right before the late season precipitation, had increased WVF levels compared to pre-clip levels. Water vapor fluxes from plots clipped on DOY 227 were similar to pre-clip levels 16 days following clipping. WVF

from both sets of plots increased and was similar to or greater than plots clipped on DOY 160 and DOY 177 for the remainder of the season.

Discussion

Of some surprise was the similar soil water content among treatments both years of the study. Previous studies in the tallgrass prairie have indicated that clipping or grazing vegetation conserves soil water (Owensby et al. 1970, Bremer et al. 2001). One potential explanation for the uniformity of soil water content was the close proximity of the soil samples to unclipped areas. The close proximity of unclipped areas would allow for lateral movement of soil water, which could have negated any treatment differences, however there were no differences in soil water amoung treatments for the 0-5 cm, 5-10 cm, 10-15 cm, and 15-20 cm depths. That may indicate that here was no lateral movement of water.

The focus of this research was to assess the impact of clipping date and natural growing season precipitation on subsequent patterns of carbon and water vapor fluxes. Clipping, by removing leaf area, always resulted in reduced GCP, NCE, and in most cases reduced R_E and WVF. Similar reductions in NCE following clipping have been reported by Dugas et al. (1999) and Novick et al. (2004) working with the grasses *Cynodon dactylon* (L.) Pers. and *Festuca arundinacea* Schreb., respectively. Novick et al. (2004) attributed the decreased NCE to loss of green leaf area and low soil water content.

Clipping has also been reported to decrease R_E (Bremer et al. 1998, Craine et al. 1999, Wan and Luo 2003). The authors concluded that factors that affect carbon availability to roots also affect soil CO_2 flux. Wan and Luo (2003) reported that clipping

reduced both root respiration and microbial respiration, of a tallgrass prairie, due to loss of carbon substrate. Because clipping removed all the leaf area, carbon for regrowth had to come from storage organs. Following severe defoliation, the storage organs become a source of carbon utilized for regrowth of the canopy instead of sink for excess photosynthate (Davidson and Milthorpe 1966, Gonzalez et al. 1989, de Visser et al. 1997).

Similarly, removal of green leaf area has also been reported to reduce subsequent WVF (Bremer et al. 2001). The authors reported grazing decreased daily evapotranspiration up to 40% compared to ungrazed canopies. They attributed the reduction in WVF to alteration of the surface energy balance. Following clipping less leaf area is available to intercept irradiance, hence transpiration is reduced.

However, following two clippings dates, R_E and WVF were not reduced. The lack of response probably resulted from high soil water content when the plots were clipped. The high level of soil moisture would allow plants to quickly increase photosynthesis, allowing for translocation of carbon belowground providing substrate for root and microbial respiration. Also, by removing leaf area, Bremer et al. (2001) reported that more irradiance reaches the soil surface. The increased irradiance acts to increase evaporation from the soil and maintain WVF even with reduced leaf area.

Net carbon exchange fluxes and GCP of canopies clipped during periods with high available soil moisture increased rapidly. Clipping and grazing have been reported to increase net photosynthetic rates of leaves initiated following defoliation (Gold and Caldwell 1990, Wallace 1990). The removal of upper leaves allows light to penetrate deeper into the canopy (Gold and Caldwell 1990). Since meristematic tissue is typically

located below the level where ungulates graze, a canopy of younger leaves develops following clipping or grazing. Gold and Caldwell (1990) concluded that the increased light penetration and greater proportion of younger leaves led to increased photosynthetic rates per unit leaf area.

However, during both years, water became limiting during some portion of the growing season, causing fluxes of carbon and water vapor to decline. While the dominant species in this study are adapted to water stress, many studies have reported the sensitivity of NCE to water stress. Knapp (1985), working with big bluestem, reported leaf photosynthetic rates approaching zero under severe water stress. Measuring net ecosystem CO_2 exchange (NEE) of an Oklahoma tallgrass prairie with eddy covariance methods, Suyker and Verma (2001) and Suyker et al. (2003) reported that water stress decreased NEE levels to near zero. The authors concluded a major influence on NEE was both the severity and timing of moisture stress.

Following late season precipitation, carbon and water vapor flux rates increased. Again, similar trends have been observed with the dominant species of the tallgrass prairie. Knapp (1985) reported that following late season precipitation, photosynthetic rates increased up to 50% of pre-drought levels. Swemmer et al. (2006), compared photosynthesis rates of wilted and well-watered big bluestem plants. The authors reported declining levels of photosynthesis as the plants approached wilting. However, following rewatering of wilted plants, photosynthetic rates increased and were similar to the well-watered big bluestem plants. Suyker and Verma (2001) and Suyker et al. (2003) also reported increasing NEE levels following rainfall.

While increases in NCE and GCP occurred for all plots following the late season precipitation, canopies that were clipped and subsequently regrew during periods of high water stress responded slower than canopies clipped during periods of adequate soil water to subsequent water availability. The limited response by canopies that developed under water stress could be caused by lack of photosynthetic apparatus or leaf area or a combination of the two. Mooney and Gulman (1979) hypothesized that the allocation of energy for photosynthesis infrastructure in plants grown in water-limited environments is less than that of plants grown in water-unlimited environments. However, a lack of leaf area could also have limited the productivity of the plants. Bacon et al. (1997) reported significant reductions in both the rate of leaf elongation and total length of drought stressed Darnel ryegrass (*Lolium temulentum* L.) plants. Durand et al. (1995) reported leaf elongation rates near zero under severe water stress. Following rewatering, two days elapsed before leaf elongation rates were similar to pre-drought rates. These results suggest that leaf expansion during periods of drought experienced in this study may have limited canopy regrowth.

Modifications to patterns of resource allocation for photosynthesis and reductions in leaf growth both appear to be explanations to the carbon flux rate patterns observed in this study. However, the design of this study did not allow for a direct comparison between the strengths of the respective impacts to subsequent carbon fluxes. To determine the degree of influence of these components carbon fluxes would need to be expressed on a per unit leaf area instead of the currently per unit ground area.

References

Atkin, O.K., M.H.M. Westbeek, M. L. Cambridge, H. Lambers, and T.L. Pons. 1997. Leaf respiration in Light and Darkness. Plant Physiology 113:961-965.

Bacon, M.A., D.S. Thompson, and W.J. Davies. 1997. Can cell wall peroxidase activity explain the leaf growth response of *Lolium temulentum* L. during drought? Journal of Experimental Botany 48:2075-2085.

Bremer, D.J., J.M. Ham, A.K. Knapp, and C.E. Owensby. 1998. Soil respiration responses to clipping and grazing in a tallgrass prairie. Journal of Environmental Quality 27:1539-1548.

Bremer, D.J., L.M. Auen, J.M. Ham, and C.E. Owensby. 2001. Evapotranspiration in a Prairie Ecosystem: Effects of Grazing by Cattle. Agronomy Journal 93:338-348.

Bremer, D.J. and J. Ham. 2002. Measurements and modeling of soil CO_2 flux in a temperature grassland under mowed and burned regimes. Ecological Applications 12:1318-1328.

Briggs, J.M. and A.K. Knapp. 1995. Interannual variability in primary production in tallgrass prairie: climate, soil moisture, topographic position, and fire as determinants of aboveground biomass. American Journal of Botany 82:1027-1030.

Brooks, A. and G.D. Farquhar. 1985. Effects of temperature on CO_2-O_2 specificity of ribulose-1,5-bisphosphate carboxylate/oxygenase and the rate of respiration in the light: estimates from gas exchange measurements on spinach. Planta 165:397-406.

Clement, C.R., M.J. Hopper, L.H.P. Jones, and E.L. Leafe. 1978. The uptake of nitrate by *Lolium perenne* from flowing nutrient solution. II. Effect of light, defoliation and relationship to CO_2 flux. Journal of Experimental Botany 29:1173-1183.

Coyne, P.I., M.J. Trlica, and C.E. Owensby. 1995. Carbon and nitrogen metabolism in range plants. In Wildland Plants: Physiological Ecology and Developmental Morphology. J.K. Meduna and R.E. Sosebee eds. Society for Range Management. Denver, CO. pp. 59-167.

Craine, J. M., D. A. Wedin, and F. S. Chapin III. 1999. Predominance of ecophysiological controls on soil CO_2 flux in a Minnesota grassland. Plant and Soil 207:77–86.

Crider, F.J. 1955. Root growth stoppage resulting from defoliation of grass. USDA Technical Bulletin 1102. U.S. Government Print. Office, Washington, DC.

Danckwerts, J.E. 1993. Reserve carbon and photosynthesis: their role in regrowth of *Themeda triandra*, a widely distributed subtropical graminaceous species. Functional Ecology 7:634-641.

Davidson, J.L. and F.L. Milthorpe. 1966. The effect of defoliation on the carbon balance in *Dactylis glomerata*. Annals of Botany 30:185-198.

Davidson, J.E. and A.J. Gordon. 1987. Long-term partitioning, storage and remobilization of 14C assimilated by *Lolium perenne* (cv. Melle). Annals of Botany 59:55-66.

de Visser R, H. Vianden, and H. Schnyder 1997. Kinetics and relative significance of remobilized and current C and N incorporation in leaf and root growth zones of *Lolium perenne* after defoliation. Assessment by ^{13}C and ^{15}N steady-state labeling. Plant Cell and Environment 20:37-46.

Dugas, W.A., M.L. Heuer, and H.S. Mayeux. 1999. Carbon dioxide fluxes over bermudagrass, native prairie, and sorghum. Agriculture and Forest Meteorology 93:121-139.

Durand, J.E., B. Onillon, H. Schnyder, and I. Rademacher. 1995. Drought effects on cellular and spatial parameters of leaf growth in tall fescue. Journal of Experimental Botany 46:1147-1155.

Gold, W. G. and M. M. Caldwell. 1990. The effects of the spatial pattern of defoliation on regrowth of a tussock grass. III. Photosynthesis, canopy structure and light interception. Oecologia 82:12–17.

Gonzales B., J. Boucaud, J. Salette, J. Langlois, and M. Duyme. 1989. Changes in stubble carbohydrate content during regrowth of defoliated perennial ryegrass (*Lolium perenne* L.) on two nitrogen levels. Grass and Forage Science 44:411-415.

Harper, C.W., J.M. Blair, P.A. Fay, A.K. Knapp, and J.D. Carlisle. 2005. Increased rainfall variability and reduced rainfall amount decreases soil CO_2 flux in a grassland ecosystem. Global Change Biology 11:322-334.

Hunt S. 2003. Measurements of photosynthesis and respiration in plants. Physiologia Plantarum 117: 314–325.

Knapp, A.K. 1985. Effect of fire and drought on the ecophysiology of *Andropogon gerardii* and *Panicum virgatum* in a tallgrass prairie. Ecology 66:1309-1320.

Knapp, A.K. and M.D. Smith. 2001. Variation amoung biomes in temporal dynamics of aboveground primary production. Science 291:481-484.

Lecain, D. R., J. A. Morgan, G. E. Schuman, J. D. Reeder, and R. H. Hart. 2000. Carbon exchange rates in grazed and ungrazed pastures in Wyoming. Journal of Range Management 53:199–206.

McKendrick, Jay D., Clenton E. Owensby, and Robert M. Hyde. 1975. Big bluestem and indiangrass vegetative reproduction and annual reserve carbohydrate and nitrogen cycles. Agro Ecosystems 2:75-93.

Mooney, H.A. and S.L. Gilmon. 1979. Environmental and evolutionary constraints on the photosynthetic characteristics of higher plants. In Topics in Plant Population Biology. O.T. Solbrig, S. Jain, G.B. Johnson, and P.H. Raven eds. Columbian University Press, New York. Pg 316-337.

Morris, J. T. and A. Jensen. 1998. The carbon balance of grazed and nongrazed *Spartina anglica* saltmarshes at Skadlingen, Denmark. Journal of Ecology 86:229–242.

Novick, K.A., P.C. Stoy, G.G. Katul, D.S Ellsworth, M.B.S Siqueira, J.Juang, and R. Oren. 2004. Carbon dioxide and water vapor exchange in a warm temperate grassland. Oecologia 138:259-274.

Ourry, A., J. Boucaud, and J. Salette. 1988. Nitrogen mobilization from stubble and roots during re-growth of defoliated perennial ryegrass. Journal of Experimental Botany 39:803-809.

Owensby, C.E., R.M. Hyde, and K.L. Anderson. 1970. Effect of clipping and added moisture and nitrogen on loamy upland bluestem range. Journal of Range Management 23:341- 347.

Owensby, C.E., E.F. Smith, and J.R. Rains. 1977. Carbohydrate and nitrogen reserve cycles for continuous, season-long, and intensive early-stocked Flint Hills bluestem range. Journal of Range Management 30:258-260.

Owensby, C.E., J.M Ham, and L.M. Auen. 2006. Fluxes of CO_2 from grazed and ungrazed tallgrass prairie. Rangeland Ecology and Management 59:111-127.

Richards, J.H. and M.M. Caldwell. 1985. Soluble carbohydrates, concurrent photosynthesis and efficiency in regrowth following defoliation: A field study with *Agropyron* species. Journal of Applied Ecology 22:907-920.

Smith, E.F. and C.E. Owensby. 1978. Intensive early-stocking and season-long stocking of Flint Hills bluestem range. Journal of Range Management 31:14-18.

Suyker, A. E. and S. B. Verma. 2001. Year-round observations of the net ecosystem exchange of carbon dioxide in a native tallgrass prairie. Global Change Biology 7:279–289.

Suyker, A.E., S.B. Verma, and G.G. Burba. 2003. Interannual variability in net CO_2 exchange of a native tallgrass prairie. Global Change Biology 9:255-265.

Swemmer, A.M., A.K. Knapp, and M.D. Smith. 2006. Growth responses of two dominant C4 grass species to altered water availability. International Journal of of Plant Sciences 167:1001-1010.

Wallace, L. L. 1990. Comparative photosynthetic responses of big bluestem to clipping versus grazing. Journal of Range Management 43:58–61.

Wan, S. and Y. Luo. 2003. Substrate regulation of soil respiration in a tallgrass prairie: Rsults of a clipping and shading experiment. Global Biogeochemical Cycles 17:1054, doi:10.1029/2002GB001971.

Wilsey, B.J., G.Parent, N.T. Roulet, T.R. Moore, and C. Potvin. 2002. Tropical pasture carbon cycling: relationships between C source/sink strength, above-ground biomass and grazing. Ecology Letters 5:367-376.

Wohlfahrt, G., M. Bahn, A. Haslwanter, C. Newesely, and A. Cernusca. 2005. Estimation of daytime ecosystem respiration to determine gross primary production of a mountain meadow. Agricultural and Forest Meteorology 130:13-25.

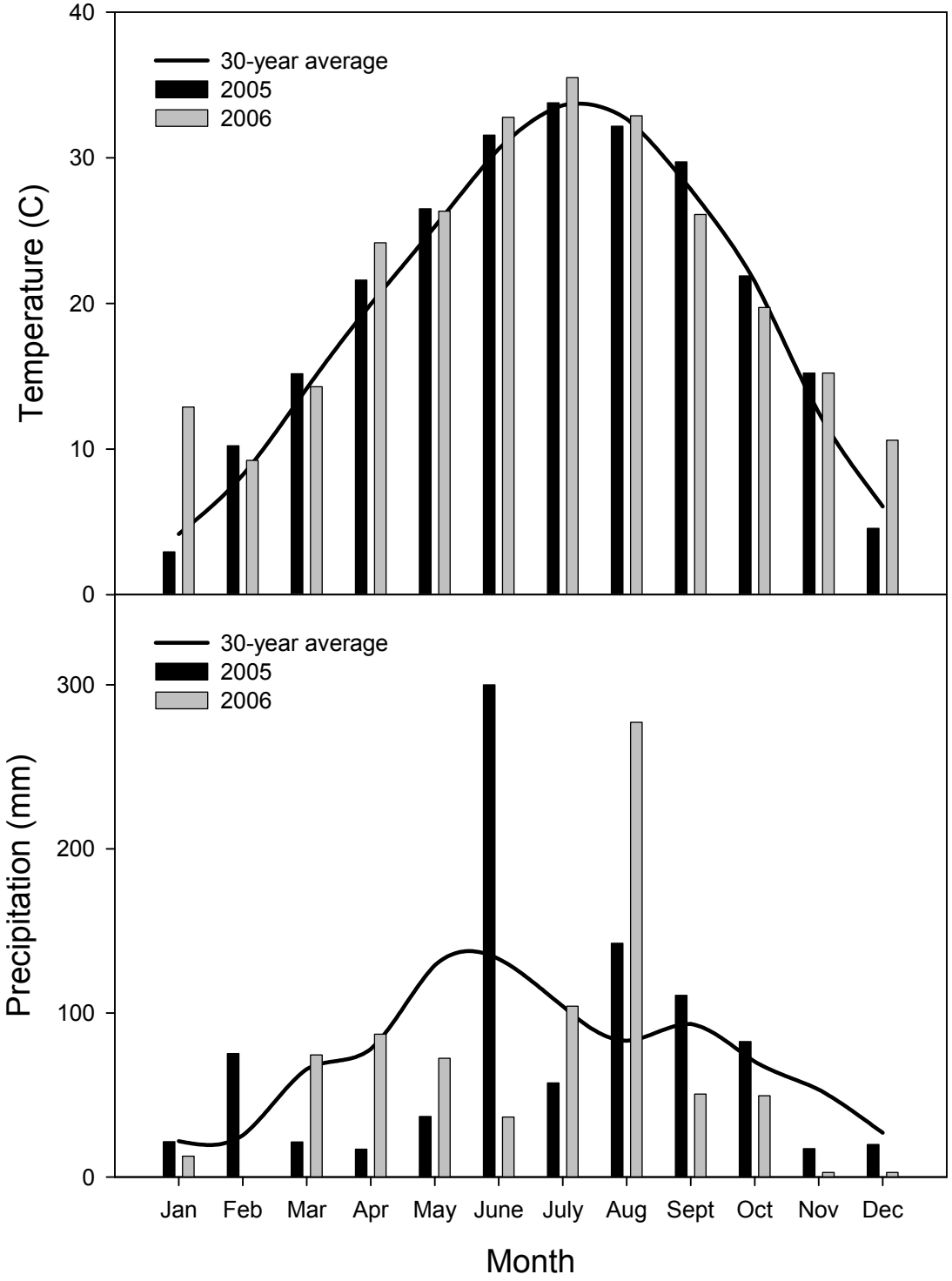

Figure 2.1. Thirty-year seasonal and average monthly temperatures for 2005 and 2006 (a) and 30-year seasonal and measured precipitation for 2005 and 2006 (b) measured from Manhattan, KS.

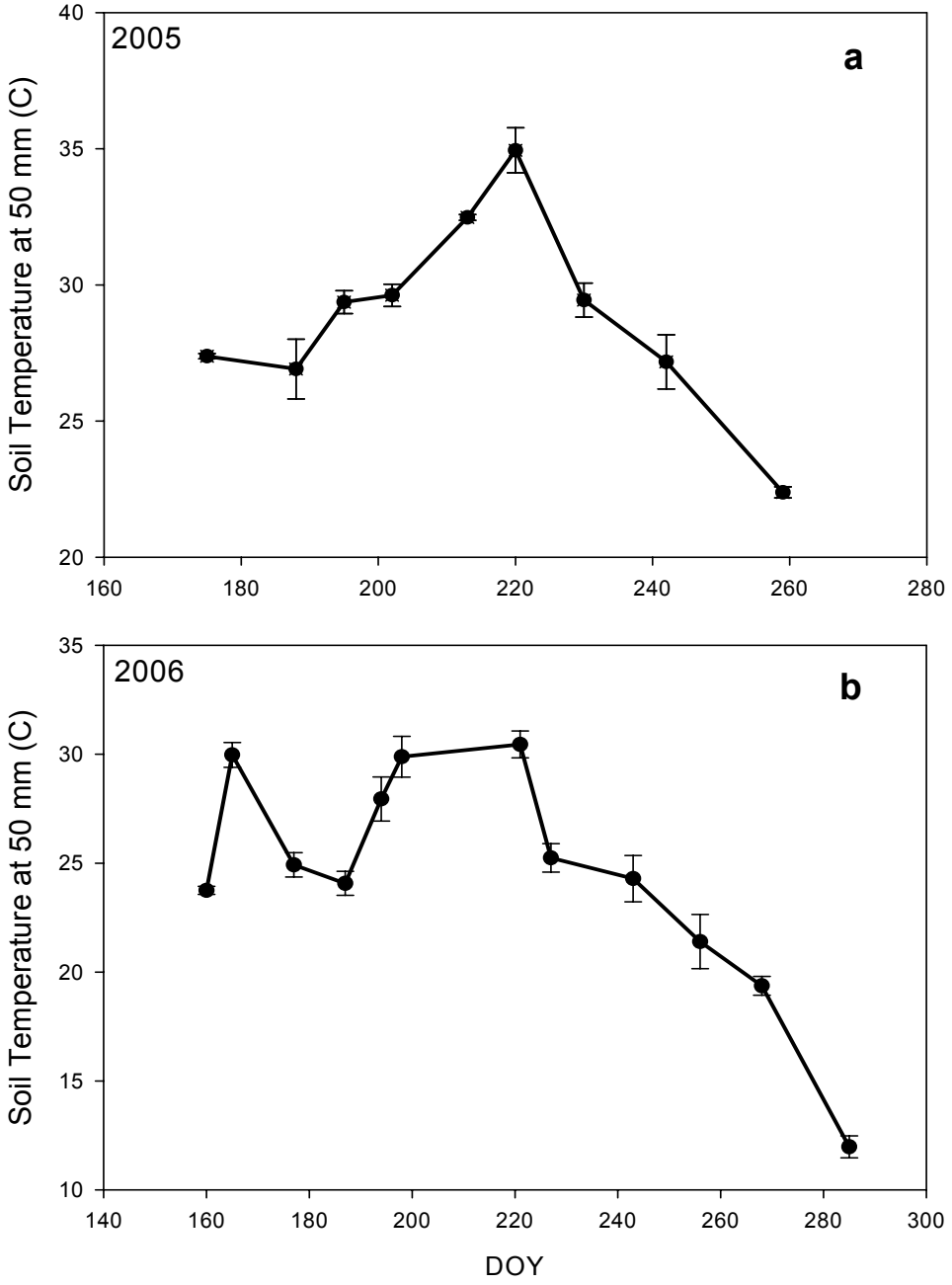

Figure 2.2. Growing season patterns of mid-day soil temperature measured at 5 cm depth from the initial clipping treatment for 2005 (a) and 2006 (b). Error bars represent 1 SE (n=3).

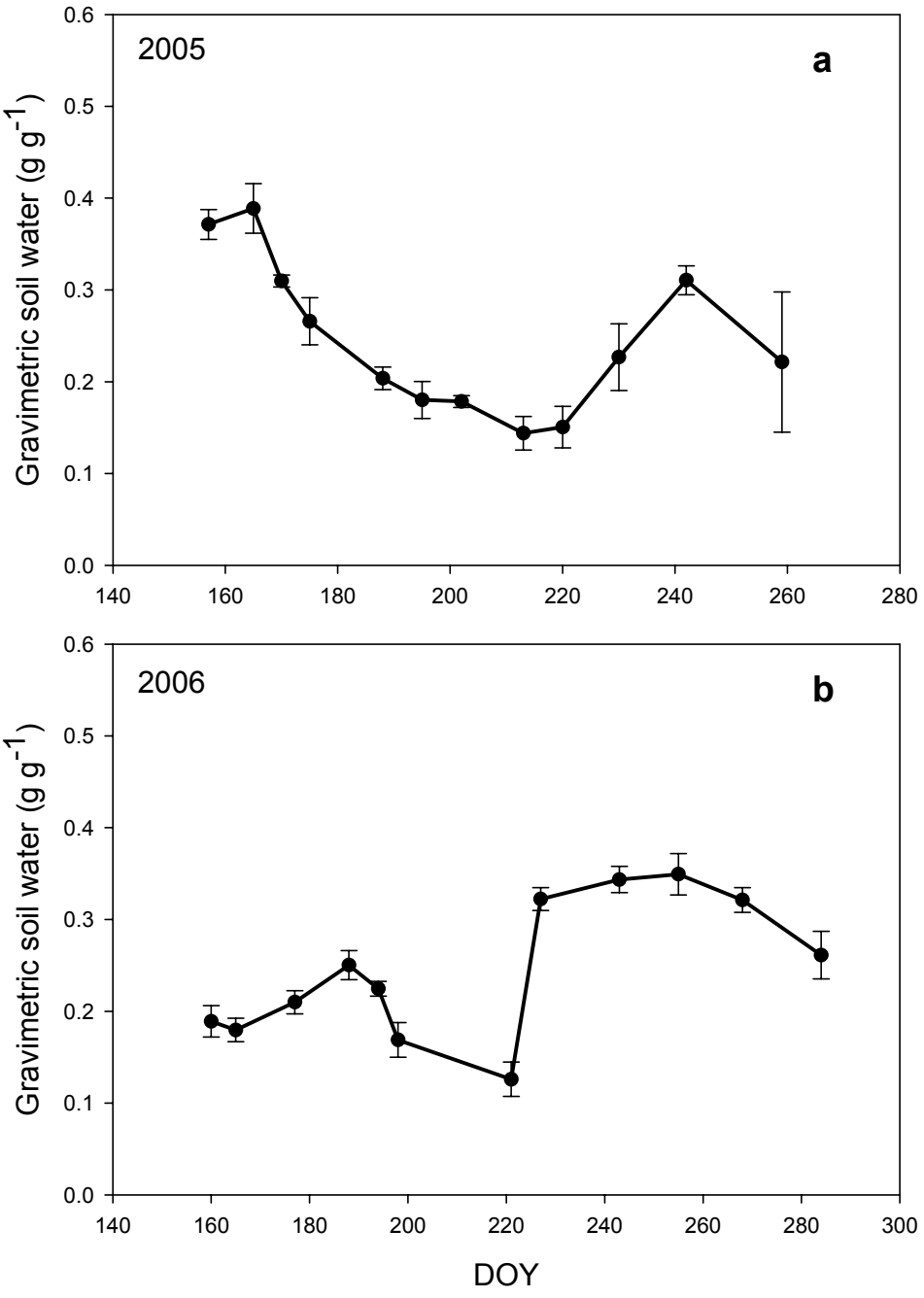

Figure 2.3. Growing season patterns of soil water content in the top 20 cm of the soil profile for 2005 (a) and 2006 (b). Error bars represent 1 SE (n=3).

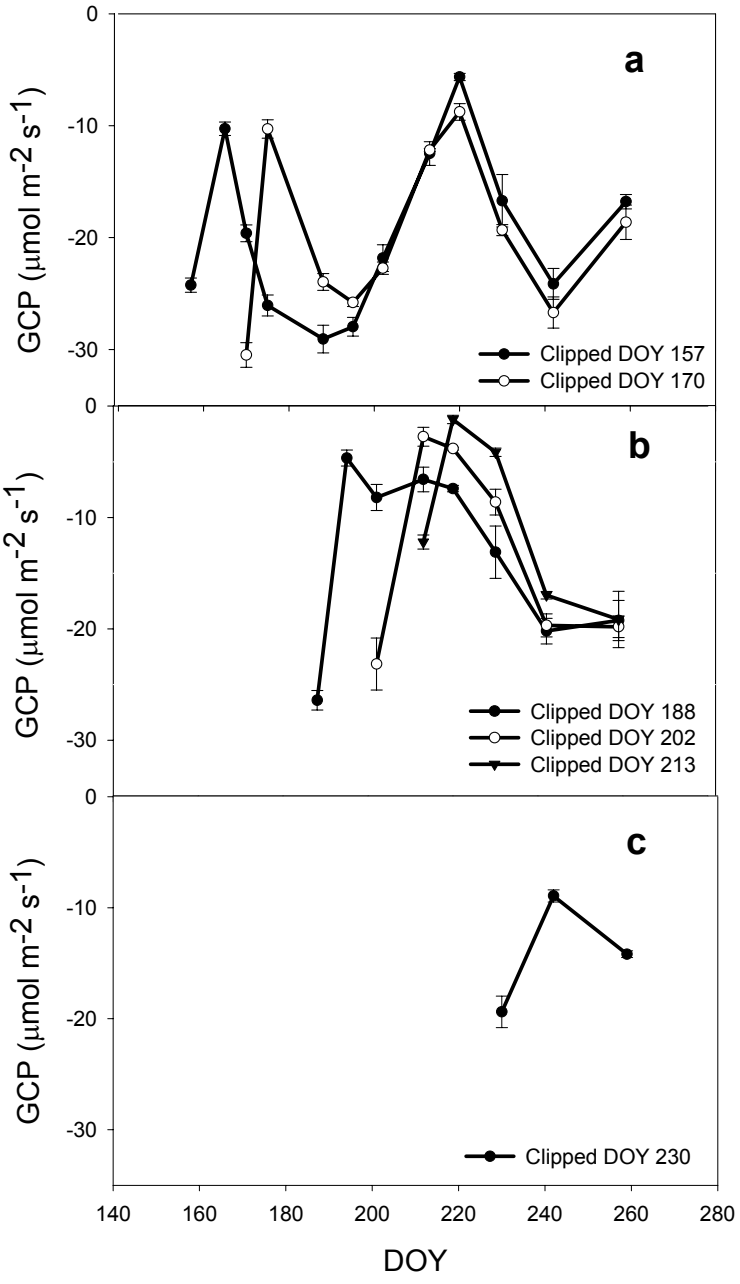

Figure 2.4. Gross canopy photosynthesis flux rates (GCP) calculated as the summation of net carbon exchange and ecosystem respiration during 2005 from plots clipped on day of year (DOY) 157 and DOY 170 (a), plots clipped on DOY 188, DOY 202, and DOY 213 (b) and plots clipped on DOY 230 (c). Error bars represent 1 SE (n=3). A negative value indicates the biosphere acting as a sink for CO_2.

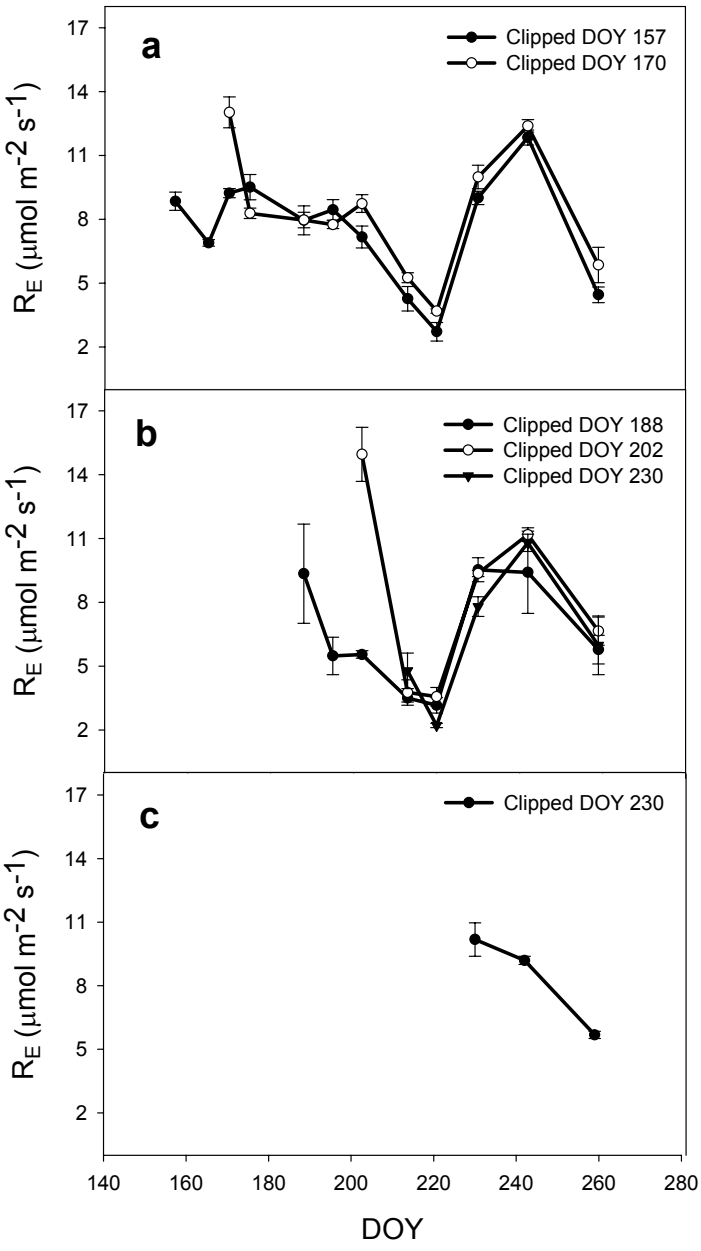

Figure 2.5. Ecosystem respiration flux rates (R_E) measured during 2005 with an opaque chamber from plots clipped on day of year (DOY) 157 and DOY 170 (a), plots clipped on DOY 188, DOY 202, and DOY 213 (b) and plots clipped on DOY 230 (c). Error bars represent 1 SE (n=3). A positive value indicates movement of CO_2 to the atmosphere.

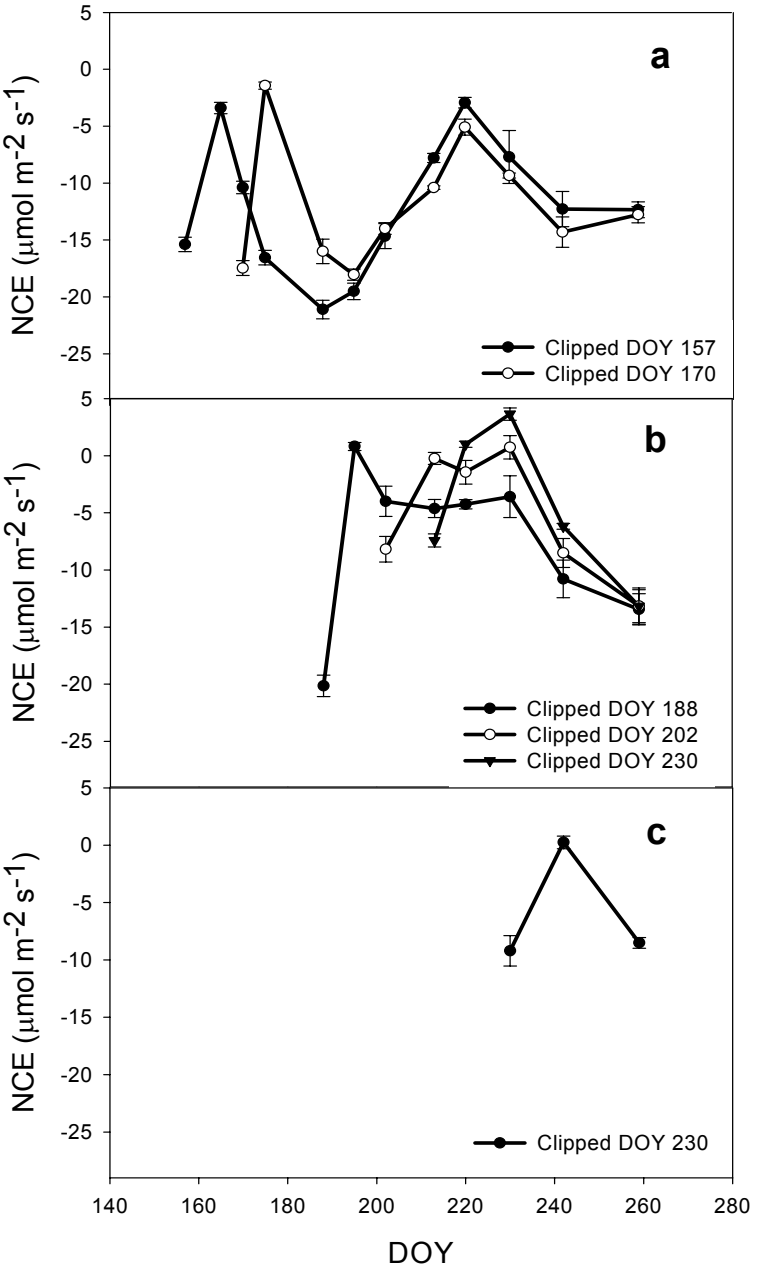

Figure 2.6. Net carbon exchange flux rates (NCE) measured during 2005 with a transparent chamber from plots clipped on day of year (DOY) 157 and DOY 170 (a), plots clipped on DOY 188, DOY 202, and DOY 213 (b) and plots clipped on DOY 230 (c). Error bars represent 1 SE (n=3). A negative value indicates the biosphere acting as a sink of CO_2.

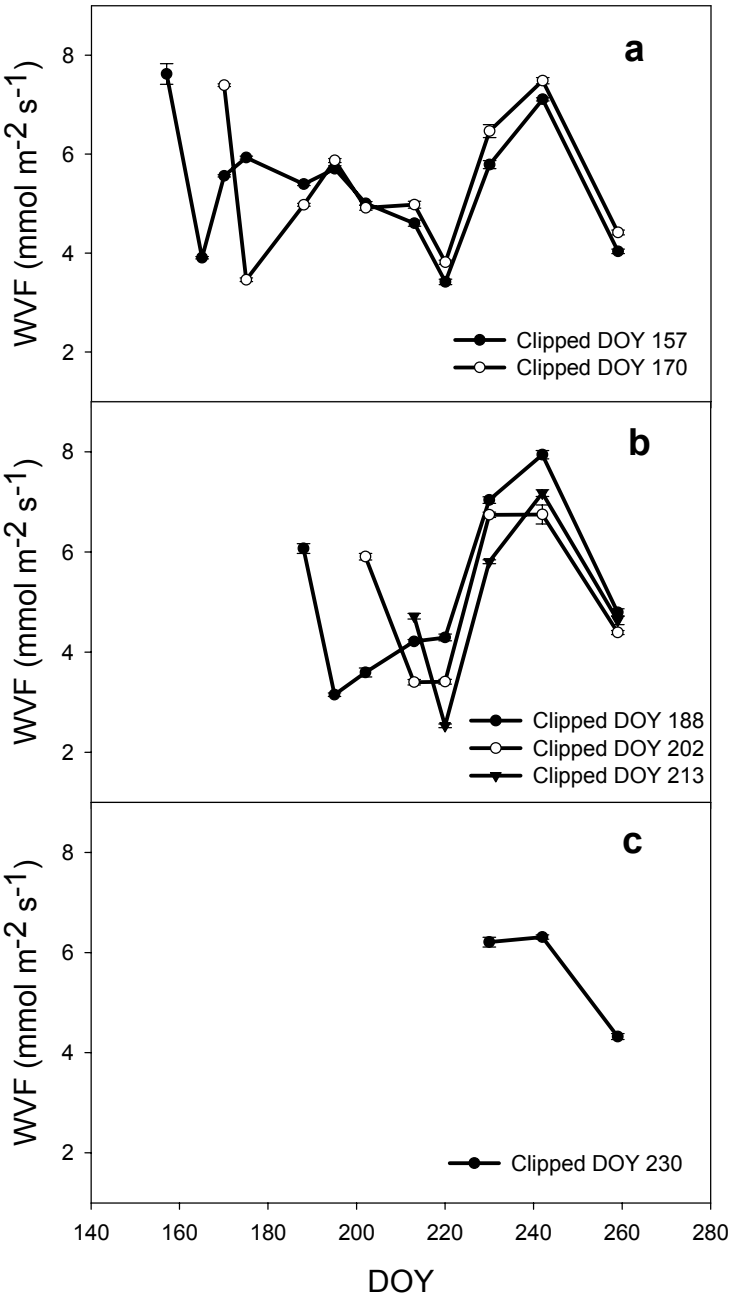

Figure 2.7. Water vapor flux rates (WVF) measured with a transparent chamber from plots clipped on day of year (DOY) 157 and DOY 170 (a), plots clipped on DOY 188, DOY 202, and DOY 213 (b) and plots clipped on DOY 230 (c). Error bars represent 1 SE (n=3). Positive value indicates movement of water vapor to the atmosphere.

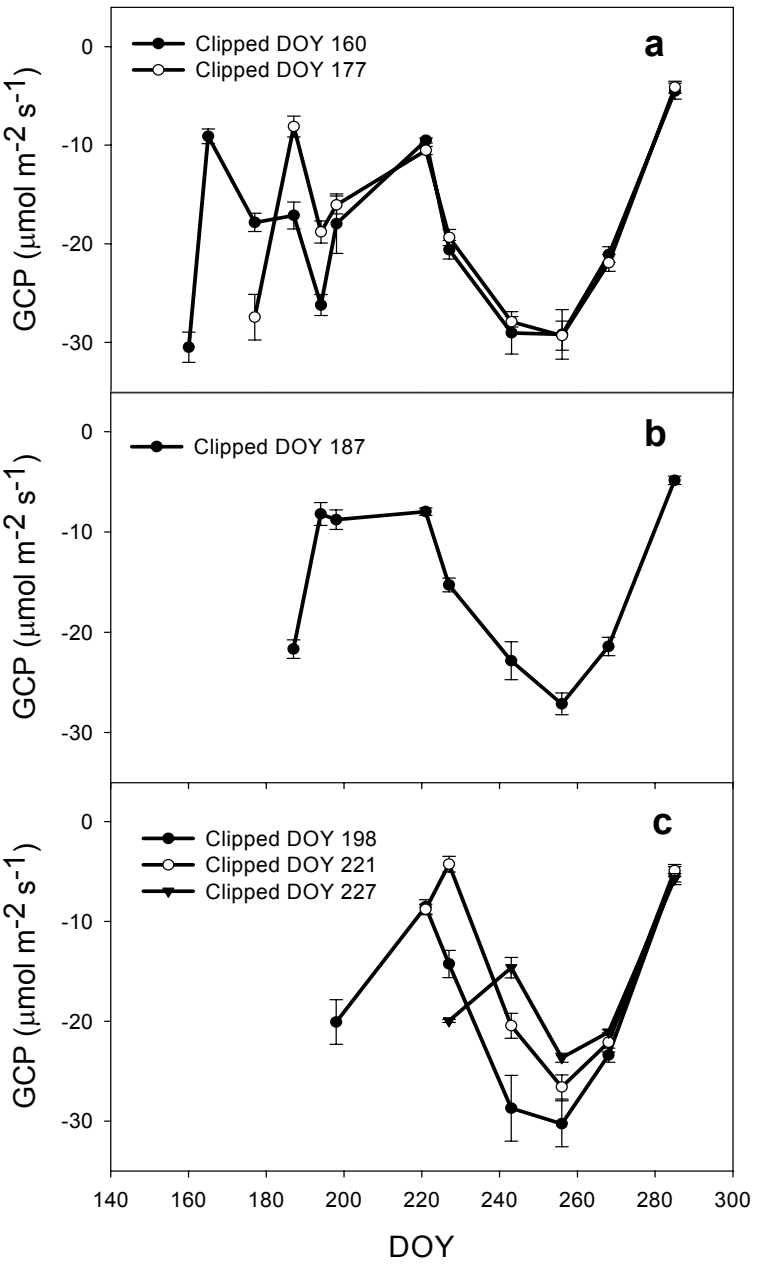

Figure 2.8. Gross canopy photosynthesis flux rates (GCP) calculated as the summation of net carbon exchange and ecosystem respiration during 2006 from plots clipped on day of year (DOY) 160 and DOY 177 (a), plots clipped on DOY 187, DOY 198 (b) and plots clipped on DOY 221 and DOY 227 (c). Error bars represent 1 SE (n=3). A negative value indicates the biosphere acting as a sink of CO_2.

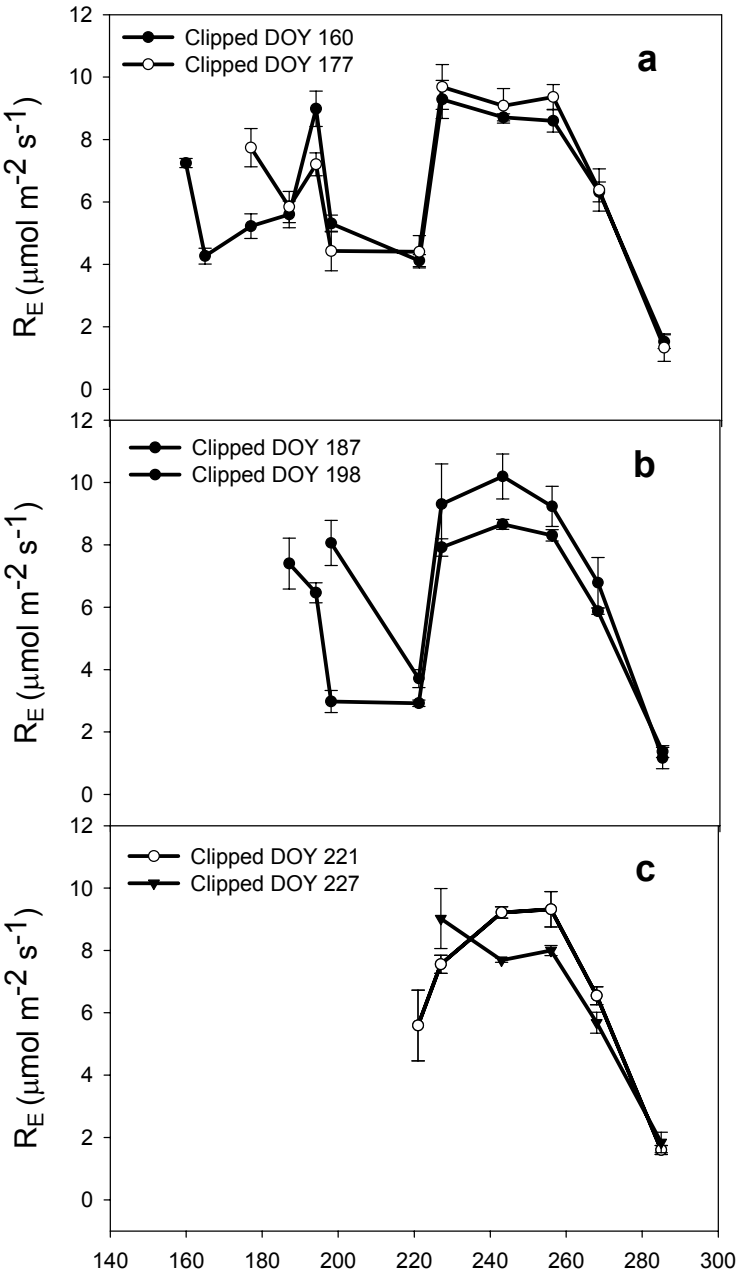

Figure 2.9. Ecosystem respiration flux rates (R_E) measured during 2006 with an opaque chamber from plots clipped on day of year (DOY) 160 and DOY 177 (a), plots clipped on DOY 187, DOY 198 (b) and plots clipped on DOY 221 and DOY 227 (c). Error bars represent 1 SE (n=3). A positive value indicates movement of CO_2 to the atmosphere.

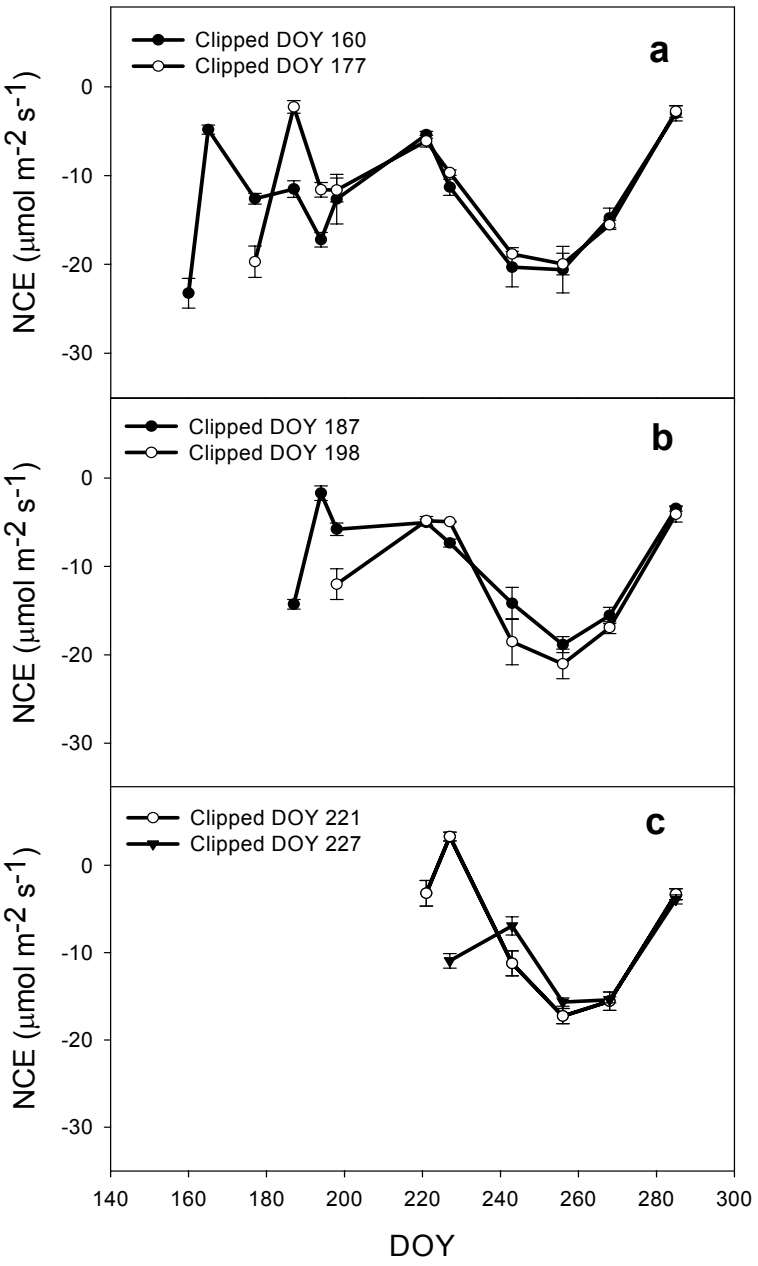

Figure 2.10. Net carbon exchange flux rates (NCE) measured during 2006 with a transparent chamber from plots clipped on day of year (DOY) 160 and DOY 177 (a), plots clipped on DOY 187, DOY 198 (b) and plots clipped on DOY 221 and DOY 227 (c). Error bars represent 1 SE (n=3). A negative value indicates the biosphere acting as a sink of CO_2.

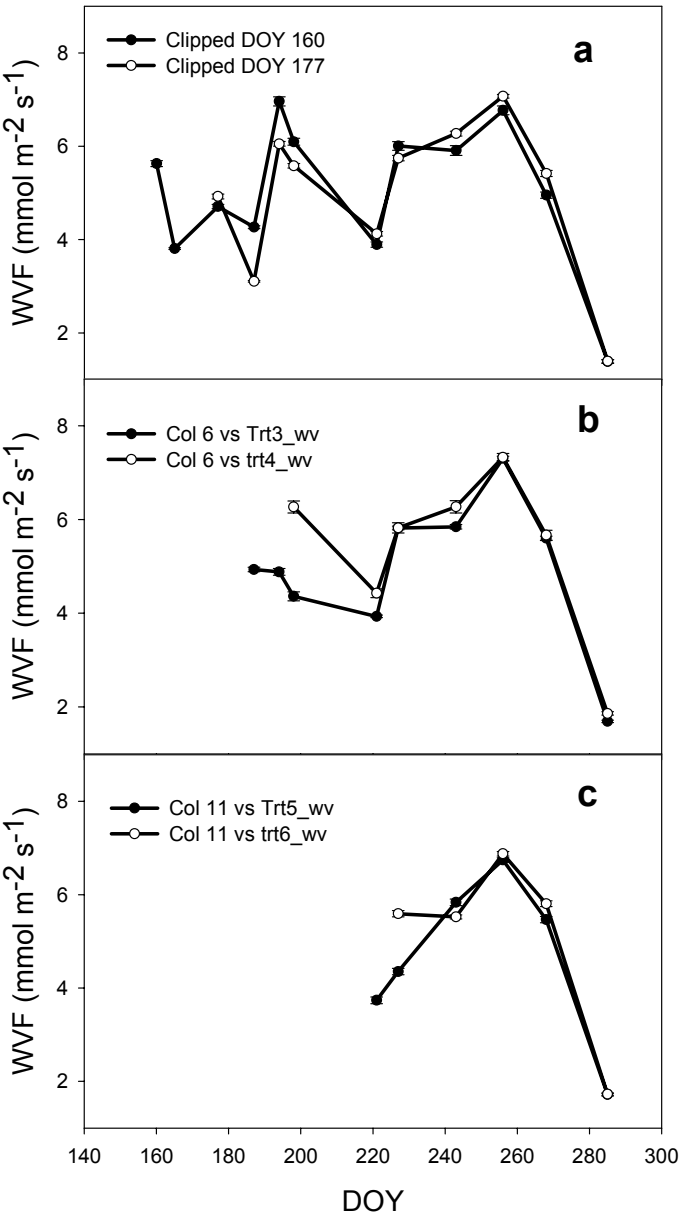

Figure 2.11. Water vapor flux rates (WVF) measured during 2006 with a transparent chamber from plots clipped on day of year (DOY) 160 and DOY 177 (a), plots clipped on DOY 187, DOY 198 (b) and plots clipped on DOY 221 and DOY 227 (c). Error bars represent 1 SE (n=3). A positive value indicates movement of water vapor to the atmosphere.

CHAPTER 3 - Estimation of Vegetative Characteristics by Remote Sensing

Abstract

Measurements of biomass, leaf area and carbon cycling rates are important components for understanding ecosystem processes. While other techniques are available to measure these components, remote sensing has the advantages of non-destructive sampling and sampling at large scales. An experiment was conducted from June through mid-October of 2006 to estimate gross canopy photosynthesis (GCP), leaf area index (LAI) and total aboveground biomass of an ungrazed tallgrass prairie with a hyperspectral radiometer and compare these estimates to flux chamber measurements. Four indices (Normalized Difference Vegetation Index (NDVI), Simple Ratio (SR), $(R_{nir}/R_{rededge})$-1, and (R_{nir}/R_{green})-1 were used to predict LAI and total biomass. Six indices (NDVI, SR, $[(R_{nir}/R_{rededge})$-1]*photosynthetically active radiation (PAR),$[(R_{nir}/R_{green})$-1]*PAR, Photochemical Reflectance Index (PRI) and the Water Band Index (WBI)) were used to derive an estimate of GCP. All indices had poor correlations to LAI and total aboveground biomass. However, GCP was significantly correlated to all six indices utilized in this study. While GCP measured from June-October was significantly correlated to all indices, removal of the October scans greatly increased the accuracy of all models except the PRI. This study demonstrates the strong relationship between GCP and spectral reflectance in the tallgrass prairie. These relationships may

be further utilized with other methods of measuring carbon exchange to gain greater understanding of larger scale ecosystem processes.

Introduction

Remote sensing has the advantages of non-destructive sampling and sampling at large scales. Hyperspectral reflectance spectra are useful for estimating vegetation characteristics such as gross canopy photosynthesis (GCP), biomass, and leaf area index (LAI). Specific wavebands within the reflectance spectra are then utilized to calculate vegetation indices, which remove error caused by soil and atmospheric conditions as well as vegetation geometry (Blackburn and Stelle 1999, Gao et al. 2000). By using these indices, large data sets can be quickly collected to provide information on carbon cycling rates, fire fuel loads, ecosystem productivity, and parameters for modeling ecosystem function.

Some commonly used vegetation indices contrast spectral reflectance in the red and infrared wavelengths and are referred to as greenness indices. These vegetation indices contrast the high absorption of red spectra by chlorophyll to the high reflectance of near infrared spectra due to scattering (Myneni et al. 1997). Two vegetation indices that utilize this relationship include the Normalized Difference Vegetation Index (NDVI) (Rouse et al. 1973) and the Simple Ratio (SR) (Birth and McVey 1968). However, the relationships between NDVI and certain vegetative characteristics (LAI and biomass) are curvilinear when LAI exceeds 2 under moderate to high biomass yields (Myneni et al. 1997). This results from the high absorption of the red wavelengths by dense canopies (Gitelson 2004).

Birth and McVey (1968) utilized the high absorption of red wavelengths and high reflectance of infrared wavelengths by green, actively growing leaves to determine the

greenness of turf grass. Jordan (1969) later used the SR to estimate LAI of a broadleaf forest in Puerto Rico.

In an attempt to circumvent the problematic saturation of the red spectra at relatively low chlorophyll contents, Gitelson et al. (2003) developed two new indices from relationships between the infrared and red-edge or green wavebands to estimate LAI and green leaf biomass. Absorption in these wavebands by chlorophyll does not saturate even at high chlorophyll content (Gitelson and Merzlyak 1994, Gitelson et al. 1996).

Gitelson and Merzlyak (2004) also demonstrated that these indices were linearly related to leaf chlorophyll content. Gitelson et al. (2006) determined the relationship between gross primary productivity and an index utilizing the estimated chlorophyll content multiplied by the photosynthetically active radiation (PAR) in uniform corn and soybean fields. While these algorithms successfully predicted GPP, LAI, and green biomass in uniform agronomic settings, the authors stressed the importance of further model validation with different crops and geographic sites (Gitelson et al. 2006).

Other vegetation indices focus on measuring physiological functions that are related to plant productivity. Two of these vegetation indices include the Photochemical Reflectance Index (PRI) (Gamon et al. 1992) and the Water Band Index (WBI) (Penuelas et al. 1993). The PRI measures the conversion of violaxanthin to antheraxanthin and zeaxanthin by de-epoxidase reactions, which allow plants to dissipate excess light as heat (Demmig-Adams and Adams 1996). The PRI is closely linked to photosystem II activity and has a high correlation with net carbon uptake from upper canopy leaves (Gamon et al. 1997).

Penuelas et al. (1993) reported a significant correlation between the WBI, relative water content, stomatal conductance, and photosynthetic rates of *Gerbera jamesonii*, *Capsicum annuum*, and *Phaeolus vulgaris*. The importance of plant water status on leaf and canopy photosynthesis has also been demonstrated for the tallgrass prairie (Knapp 1985, Suyker and Verma 2001, Suyker et al. 2003).

However, the relationships between vegetation indices and GCP, LAI, and biomass are influenced by plant species, leaf type, canopy architecture and geographic region and water status and some newer indices have only been tested on a few species (Billings and Morris 1951, Clark and Lister 1975, Reicosky and Hanover 1978, Gitelson et al. 2006).

The objective of this research was to use reflectance spectra to assess the relationships among various vegetative indices, LAI, biomass, and GCP of a tallgrass prairie throughout the growing season.

Materials and Methods

Study Area

The study was conducted from June through October during 2006. The site was an ungrazed pasture located in the Rannells Flint Hills Prairie Preserve, 5-km south of Manhattan, KS (39.11°N, 96.34°W, 324 m above sea level). The dominant vegetation consisted of the C4 species *Andropogon gerardii* Vitman and *Sorghastrum nutans* (L.) Nash while subdominants included *A. scoparius* Michx. and *Bouteloua curtipendula* (Michx.) Kunth. The remainder of the vegetation consisted of various sedges (C3), and C3 forbs including *Vernonia baldwinii* (Small) Schub., *Ambrosia psilostachya* DC.,

Artemesia ludoviciana Nutt., and *Psorelea tenuiflora* var. floribunda (Nutt.) Rydb. The soil was a Dwight silty clay (Fine, smectitic, mesic Typic Natrustolls) on a 1-3% slope. Average annual precipitation (1971-2000) is 884 mm with 542 mm (61%) occurring from May through September. Eighteen plots were established in mid-May of 2006 by pressing 0.85 m x 0.85 m soil collars into the soil. The soil collars were constructed of 5.1 cm x 7.6 cm x 0.5 cm angle iron into the soil until the top was 5 cm above the soil surface.

Measurements of CO_2 Fluxes

Net carbon exchange flux (NCE) and Ecosystem Respiration (R_E) were measured with a non-steady-state closed system chamber (Murphy 2007; Chap. 1). The chamber footprint was 0.85-m x 0.85-m with a height of 0.25 m and total weight of 10.9 kg. Sides were constructed of 4.59-mm acrylic-FE (Acrylite, Cyro Industries, Clifton, NJ). The top was made from heat-stretched Propafilm-C (ICI Americas Inc., Wilmington, DE) with high thermal and visible transmittance (Hunt 2003). A closed-cell foam gasket (nomapack-WS, Nomaco Inc, Zebulon, NC) provided a tight seal between the bottom edges of the chamber sides and the soil collar. Two fans (700 L min-1, BD 12A3, Comair Rotron, San Diego, CA) circulated air through a perforated plenum attached to the inside wall near the bottom of the chamber. The rate change of CO_2 concentration within the chamber was measured with a closed path infrared gas analyzer (IRGA, LI-840, Li-Cor Industries, Lincoln, NE). Net carbon exchange was measured with the chamber exposed to ambient light. Chamber measurements were initiated by recording ambient conditions above the canopy for 20 seconds. Data acquisition was then paused for five seconds while the chamber was positioned over the canopy and placed onto the

soil frame. Following the five-second pause, data acquisition resumed for a 40-second period with the chamber positioned over the canopy. Following each reading, the chamber was removed from the canopy and the CO_2 and water vapor concentrations and air temperature within the chamber were allowed to equilibrate with ambient conditions. Ecosystem respiration was then measured by excluding light with an opaque chamber positioned over the canopy. The sampling procedure was the same for NCE. Gross Canopy Photosynthesis (GCP) is the sum of net carbon exchange (NCE) and ecosystem respiration (R_E)

$$GCP = NCE + R_E \qquad \text{[eq. 3.1]}$$

with all terms in μmol m^{-2} s^{-1}. The micrometeorological convention of labeling fluxes from the ecosystem to the atmosphere as positive (source of CO_2) was utilized in this study.

Reflectance Measurements

Following the measurements of NCE and R_E, a dual-channel field spectrophotometer (Unispec-DC, PP Systems, Haverhill, MA) was utilized to record reflectance from the same plots used for the chamber measurements. The Unispec-DC consists of two spectrophotometers that measure reflectance between 310-1100 nm in 3.3 nm bandwidths, for a total of 256 data points collected per scan. One spectrophotometer, with a 12° field of view foreoptic, sampled upwelling radiation from the target while the second spectrophotometer had a hemispherical diffuser foreoptic that measured incoming irradiance. Both spectrophotometers were mounted on a tripod 1.5 m above the ground, which resulted in 0.07-m^2 view, 10% of the total plot area.

Prior to each scanning period, a two-step process calibrated the two spectrophotometers. First, a dark scan was conducted by completely blocking all radiation to the instrument. The dark scan removes sensor noise that is associated with the temperature of the spectrophotometers. The two spectrophotometers were then calibrated using a barium sulfate panel by comparing upwelling radiance measured from the panel to irradiance measured by the cosine diffuser.

A linear interpolation of the reflectance spectra was performed (Multspec 5.1, available from Specnet.info) that calculated values in 1 nm increments. These interpolated values were then used to calculate the vegetation indices.

Spectral Indices

The two greenness indices, NDVI and SR, which are based on contrasting the absorption in the red and infrared regions of the spectrum were calculated as:

$$NDVI = \frac{(R_{800} - R_{680})}{(R_{800} + R_{680})} \qquad \text{[eq. 3.2]}$$

$$SR = \frac{R_{800}}{R_{680}} \qquad \text{[eq. 3.3]}$$

where R_{800} and R_{680} are reflectance values recorded in the infrared and red wavelengths, respectively.

The two indices developed by Gitelson et al. (2003) to predict LAI and green biomass using the relationships among wavebands that do not saturate at high biomass and LA were calculated as:

$$\frac{R_{840-870}}{R_{700-730}} - 1 \qquad \text{[eq. 3.4]}$$

$$\frac{R_{840-870}}{R_{545-565}} - 1 \qquad \text{[eq. 3.5]}$$

where $R_{xxx\text{-}xxx}$ is the average reflectance value of the spectra within the denoted wavebands. The relationships between GCP was then estimated using:

$$\left[\frac{R_{840-870}}{R_{700-730}} - 1\right] * PAR \qquad \text{[eq. 3.6]}$$

$$\left[\frac{R_{840-870}}{R_{545-565}} - 1\right] * PAR \qquad \text{[eq. 3.7]}$$

where $\frac{R_{840-870}}{R_{700-730}} - 1$ and $\frac{R_{840-870}}{R_{545-565}} - 1$ are measures of the chlorophyll concentration as defined by Gitelson et al. (2005). Photosynthetically active radiation was measured with a quantum sensor (LI-190, LiCor Industries, Lincoln, NE) .

The PRI, a reflection index that can be used to estimate xanthophyll concentration, was calculated as:

$$PRI = \frac{(R_{531} - R_{570})}{(R_{531} + R_{570})} \qquad \text{[eq. 3.8]}$$

where R_{531} is an estimate of xanthophyll concentration, while R_{570} is a reference band where absorption is not due to xanthophylls.

The WBI index value was calculated as:

$$WBI = \frac{R_{900}}{R_{970}} \qquad \text{[eq. 3.9]}$$

where R_{970} is a wavelength absorbed by water and R_{900} is a reference wavelength outside the water absorption band.

Pearson's correlation analysis was performed to test the relationships between LAI, biomass, and equations 1-4, while equations 1, 2, 5, 6, 7, and 8 were tested

against GCP (Proc Corr, SAS 9.1, SAS Institute, Cary, NC). Linear regression was then performed to determine the coefficients of determination and the equation describing the relationships (Proc Reg, SAS 9.1).

Aboveground Biomass and Leaf Area Sampling

Following reflectance measurements, aboveground biomass and leaf area were determined at seven different times during the year by clipping to a height of 5 cm all of the vegetation within the plots used for both the chamber and hyperspectral measurements. The vegetation was then placed in an insulated container and transported to the laboratory where green and senesced vegetation was manually sorted. Green leaf area was measured for both graminoids and forbs with an area meter (Li-3100, Li-Cor, Lincoln, NE). Total aboveground biomass was determined gravimetrically after drying the vegetation at 55°C for 72 hrs. Total biomass was used in the calculation of the indices used for biomass estimation.

Results

Gross Canopy Photosynthesis Fluxes (GCP) and Vegetation Indices

Ninety-nine hyperspectral scans were taken from June through October over plots with GCP ranging from –3.0 to –34.4 mmol m^{-2} s^{-1}. The Pearson's correlation analysis indicated that all indices were significantly correlated with GCP (Table 3.1). The WBI and PRI had the highest correlation with GCP while [(R_{nir}/R_{green})-1] * PAR and NDVI had the lowest correlation with GCP. The results of the linear regression analysis determined that only the WBI and PRI had coefficients of determination greater than

0.56 (Fig 3.1a,b,c,d,e,f). The [(R_{nir}/R_{green})-1] * PAR index had the lowest coefficient of determination.

One interesting feature was the presence of 18 outlier scans for all indices except PRI (Fig. 3.1a,b,c,d,e,f). The outliers represent a set of hyperspectral scans that were collected on October 12, when canopies had begun senescing. Removal of these scans increased the Pearson's correlation coefficients for all vegetation indices except the PRI.

Following the removal of the outlier scans, the [($R_{nir}/R_{rededge}$)-1] * PAR index had the highest correlation coefficient, while the PRI had the lowest correlation coefficient (Table 3.1). The coefficients of determination were greater than 0.56 for all comparisons except the PRI (Figure 3.2a,b,c,d,e,f). Four indices had coefficients of determination values ≥ 0.75.

Leaf Area Index (LAI) and Vegetation Indices

Thirty-six hyperspectral scans were taken from June through October over plots with LAIs ranging from 0.28 to 2.12 m^2 m^{-2}. A Pearson's correlation analysis indicated that the SR, NDVI, and ($R_{nir}/R_{rededge}$)-1 were significantly correlated to LAI (Table 3.1). Regression analysis indicated that the SR index had the highest coefficient of determination (Fig. 3.3a,b,c,d) among the three indices. Similar to the GCP regression analysis, hyperspectral scans taken during October clustered together. Again, removal of the 18 October scans improved both the Pearson's correlation coefficients and coefficients of determination for all vegetation indices (Table 3.1).

The correlation analysis of the June to August data indicated all were significantly correlated to LAI (Table 3.1). The (R_{nir}/R_{green})-1 and ($R_{nir}/R_{rededge}$)-1 indices had the

highest correlation coefficients, while SR had the lowest correlation coefficient. Linear regression analysis indicated that all models were significant, however, the coefficients of determination were considerably lower for LAI than GCP (Fig 3.4a,b,c,d).

Total Biomass and Vegetation Indices

Thirty-six hyperspectral scans were taken from June through October over plots with biomass ranging from 45.4 to 317.6 g m^{-2}. Of the indices utilized, only the $(R_{nir}/R_{rededge})$-1 index was determined to be significantly correlated to biomass by the Pearson's correlation analysis (Table 3.1). The results of the linear regression analysis showed that while significant ($p = 0.04$), the coefficient of determination was only 0.12.

Interestingly, following removal of the October spectral scans; none of the vegetation indices were significantly correlated to biomass (Table 3.1). The coefficients of variation ranged from minimum value of 0.069 for the SR index to a maximum value of only 0.132 for the $(R_{nir}/R_{rededge})$-1 index.

Discussion

Surprisingly, all indices tested against LAI and biomass had poor correlations. Olson and Cochran (1989) and Villarreal et al. (2006), working in the tallgrass prairie, also reported weak relationships between NDVI and biomass. However, using the $(R_{nir}/R_{rededge})$-1 and (R_{nir}/R_{green})-1 indices, Gitelson et al. (2003) reported R^2's of 0.98 and 0.96 for green leaf biomass and LAI, respectively. The considerably better correlations to biomass and LAI reported by Gitelson et al. (2003) are most likely reflect the more uniform field conditions, fertilization, measurement of an annual plant, and comparison to only green leaf biomass. The agronomic field setting resulted in a more

uniform plant distribution. Unlike the fertilized, annual corn and soybean plants of Gitelson et al. (2003), that continue to partition nitrogen to the leaves, the Flint Hills is a nitrogen-limited environment (Owensby et al. 1970), and big bluestem and indiangrass, two dominant perennial grass species present in this study, conserve nitrogen by remobilizing the nitrogen from the leaves to the rhizomes during July (McKendrick et al. 1975, Owensby et al. 1977, Hayes 1985). That nitrogen is utilized to initiate growth the following spring. As the nitrogen is translocated from the leaves, chlorophyll content declines, and hence indices that utilize chlorophyll content will poorly predict LAI and biomass. Gitelson et al. (2003) further improved accuracy of the biomass model by limiting the spectral indices to only green leaf biomass instead of total biomass as used in this study. Gamon et al. (1995) reported increased correlation coefficients when NDVI and SR were regressed against only green leaf biomass instead of total standing biomass.

All of the vegetation indices utilized during this study are related to GCP measured from June through October. However, for all but one index, the 18 scans taken during October decreased the strength of the GCP-index relationship and were clustered away from the remaining 81 scans representing June through September. Removal of the 18 October scans markedly improved the coefficients of determination for all indices except PRI. The increased correlation after removal of these scans most likely resulted from a large amount of senesced grass present in October. Because chlorophyll breaks down faster during senescence than xanthophyll (Gitelson and Merzlyak 1994, Merzlyak et al. 1999) an index that measures xanthophyll appears to be better correlated to GCP than chlorophyll indices late in senescing canopies.

One surprising result of removing the October scans was the strong relationship between $[(R_{nir}/R_{rededge})-1] * PAR$ index and GCP. In monoculture stands of corn and soybean, Gitelson et al. (2004) reported a maximum $R^2 = 0.85$ for a net ecosystem exchange $[(R_{nir}/R_{rededge})-1] * PAR$ relationship, only slightly greater than that reported in this study in a heterogeneous ecosystem.

The high correlations between NDVI-GCP and SR-GCP were another unexpected finding since both indices were not related to biomass and only moderately related to LAI. The strength of the relationship is probably due to the allocation of nitrogen to the upper canopy leaves. Schimel et al. (1991), working in the tallgrass prairie, reported that nitrogen was preferentially allocated to the upper canopy leaves and that photosynthetic rates of those leaves was up to 3.2 times greater on the top canopy leaves than the lower leaves. If the majority of photosynthesis is occurring in the upper portion of the canopy, less self-shading of the most photosynthetically active leaves will occur and a better estimate of chlorophyll or greenness of the leaf is possible, which will increase the strength of the correlations to GCP.

The high R^2 of the WBI further confirms the importance of water on GCP. Knapp (1985), working with big bluestem, the dominant plant species in this study, reported leaf photosynthetic rates approaching zero under severe water stress. Hence, a measure of moisture stress should have good predictability of GCP.

Conclusions

The relationships between GCP and the vegetation indices utilized in this study demonstrate that that spectral reflectance measured by a hyperspectral radiometer can accurately estimate seasonal GCP from a tallgrass prairie. The results also indicate that

indices developed in uniform, monoculture agronomic field settings can be successfully applied to much more heterogeneous environments. However, none of the indices utilized were able to satisfactorily estimate either LAI or biomass.

The strong relationship between GCP and spectral reflectance in the tallgrass prairie further stresses the importance of integrating remote sensing and flux measurements as proposed by Gamon et al. (2006). Further work is needed to test the applicability of using remote sensing at the scale of landscape fluxes. Also, further work is needed in developing vegetation indices that better estimate LAI and biomass, which are critical for a complete understanding of landscape scale processes.

References

Aase, J.K., A.B. Frank, and R.J. Lorenz. 1987. Radiometric reflectance measurements of northern great plains rangeland and crested wheatgrass pastures. Journal of Range Management 40:299-302.

Billings, W.D. and R.J. Morris. 1957. Reflection of visible and infrared radiation from leaves of different ecological groups. American Journal of Botany 38:327-331.

Birth, G.S. and G.R. McVey. 1968. Measuring the color of growing turf with a reflectance spectrophotometer. Agronomy Journal 60:640-643.

Blackburn, G.A. and D.M. Steele. 1999. Towards the remote sensing of matorral vegetation physiology: relationships between spectral reflectance, pigment, and biophysical characteristics of semiarid bushland canopies. Remote Sensing of Environment 70:278-292.

Clark, J.B. and G.R. Lister. 1975. Photosynthetic action spectra of trees. II. The relationship of cuticle structure to the visible and ultraviolet spectral properties of needles from four coniferous species. Plant Physiology 55:407-413.

Claudio, H.C., Y. Cheng, D.A. Fuentes, J.A. Gamon, H. Luo, W. Oechel, H.L. Qui, A.F. Rahman, and D.A. Sims. 2006. Monitoring drought effects on vegetation water content and fluxes in chaparral with the 970 nm water band index. Remote Sensing of Environment 103:304-311.

Demming-Adams, B. and W.W. Adams III. 1996. The role of xanthophyll cycle carotenoids in the protection of photosynthesis. Trends in Plant Science 1:21-26.

Filella, I. J. Penuelas, L. Llorens, and M. Estiarte. 2004. Reflectance assessment of seasonal and annual changes in biomass and CO_2 uptake of a Mediterranean shrubland submitted to experimental warming and drought. Remote Sensing of Environment 90:308-318.

Gamon, J.A., J. Penuelas, and C.B. Field. 1992. A narrow waveband spectral index that tracks diurnal changes in photosynthetic efficiency. Remote Sensing of Environment 4:35-44.

Gamon, J.A., C.B. Field, M.L. Goulden, K.L. Griffin, A.E. Hartley, G. Joel, J. Penuelas, and R. Valentini. 1995. Relationships between NDVI, canopy structure, and photosynthesis in three Californian vegetation types. Ecological Applications 5:28-41.

Gamon, J.A., L. Serrano, and J.S. Surfus. 1997. The photochemical reflectance index: an optical indicator of photosynthetic radiation use efficiency across species, functional types, and nutrient levels. Oecologia 112:492-501.

Gamon, J.A., A.F. Rahman, J.L. Dungan, M. Schildhauer, and K.F. Huemmrick. 2006. Spectral Network (SpecNet) - What is it and why do we need it? Remote Sensing of Environment 103:227-235.

Gao, S., A.R. Huete, W. Ni, and T. Miura. 2000. Optical-biophysical relationships of vegetation spectra without background contamination. Remote Sensing of Environment 74:609-620.

Gitelson, A.A. and M. Merzlyak. 1994. Spectral reflectance changes associated with autumn senescence of *Aesculus hippocastanum* and *Acer platanoides* leaves. Spectral features and relation to chlorophyll estimation. Journal of Plant Physiology 143:286-292.

Gitelson, A., Y. Kaufman, and M. Merzlyak. 1996. Use of a green channel in remote sensing of global vegetation from EOS-MODIS. Remote Sensing of Environment 58:289-298.

Gitelson, A. A., A. Viña, T. J. Arkebauer, D. C. Rundquist, G. Keydan, and B. Leavitt. 2003. Remote estimation of leaf area index and green leaf biomass in maize canopies. Geophysical Research Letters 30:1248 doi:10.1029/2002GL016450.

Gitelson, A.A., and M. N. Merzlyak. 2004. Non-destructive assessment of chlorophyll, carotenoid and anthocyanin content in higher plant leaves: Principles and algorithms. Remote Sensing for Agriculture and Environment (S. Stamatiadis, J.M. Lynch, J.S. Schepers Eds.). Greece, Ella. Pg. 78-94.

Gitelson, A. A. 2004. Wide dynamic range vegetation index for remote quantification of biophysical characteristics of vegetation. Journal of Plant Physiology 161:165-173.

Gitelson, A. A., A. Viña, S. B. Verma, D. C. Rundquist, T. J. Arkebauer, G. Keydan, B. Leavitt, V. Ciganda, G. G. Burba, and A. E. Suyker. 2004. Remote estimation of net ecosystem CO_2 exchange in crops: Principles, technique calibration and validation. 2nd International Workshop on Remote Sensing of Vegetation Fluorescence. November 17-19, 2004, Montreal, Canada. CD-Rom, ESA WPP-242.

Gitelson, A.A., A. Vina, V. Diganda, D.C. Rundquist, and T.J. Arkebauer. 2005. Remote estimation of canopy chlorophyll content in crops. Geophysical Research Letters 32:L08403, doi:10.1029/2002GL016543.

Gitelson, A. A., A. Viña, S. B. Verma, D. C. Rundquist, T. J. Arkebauer, G. Keydan, B. Leavitt, V. Ciganda, G. G. Burba, and A. E. Suyker. 2006. Relationship between gross primary production and chlorophyll content in crops: Implications for the synoptic monitoring of vegetation productivity, Journal of Geophysical Research 111, D08S11, doi:10.1029/2005JD006017.

Hayes, D.C. 1985. Seasonal nitrogen translocation in big bluestem during drought conditions. Journal of Range Management 38:406-410.

Hunt, S. 2003. Measurements of photosynthesis and respiration in plants. Physiologia Plantarum 117: 314–325.

Jordan, C. F. 1969. Derivation of leaf area index from quality of light on the forest floor. Ecology 50:663-666.

Knapp, A.K. 1985. Effect of fire and drought on the ecophysiology of *Andropogon gerardii* and *Panicum virgatum* in a tallgrass prairie. Ecology 66:1309-1320.

McKendrick, J.D., C.E. Owensby, and R.M. Hyde. 1975. Big bluestem and indiangrass vegetative reproduction and annual reserve carbohydrate and nitrogen cycles. Agro-Ecosystems 2:75-93.

Merzlyak, M.N., A.A. Gitelson, O.B. Chivkunova, and V.Y. Rakitin. 1999. Non-destructive optical detection of pigment changes during leaf senescence and fruit ripening. Physiologia Plantarum 106:135-141.

Myneni, R.B., R.R. Nemani, and S.W. Running. 1997. Estimation of global leaf area index and absorbed PAR using radiative transfer models. IEEE Transactions on Geoscience and Remote Sensing 35:12380-1393.

Olson K.C. and R.C. Cochran. 1989. Radiometry for predicting tallgrass prairie biomass using regression and neural models. Journal of Range Management 51:186–192.

Owensby, C.E., R.M. Hyde and K.L. Anderson. 1970. Effect of clipping and added moisture and nitrogen on loamy upland bluestem range. Journal of Range Management 23:341-347.

Owensby, C.E., E.F. Smith, and J.R. Rains. 1977. Carbohydrate and nitrogen reserve cycles for continuous, season-long, and intensive early-stocked Flint Hills bluestem range. Journal of Range Management 30:258-260.

Penuelas, J., E. Filella, C. Biel, L. Serrano, and R. Save. 1993. The reflectance at the 950-970 nm region as an indicator of plant water status. International Journal of Remote Sensing 14:1887-1905.

Reicosky, D.A. and J.W. Hanover. 1978. Physiological effects of surface waxes. I. Light reflectance for glaucous and nonglaucus *Picea pungens*. Plant Physiology 62:101-104.

Rouse, J. W., R.H. Haas, J.A. Schell, and D.W. Deering. 1973. Monitoring vegetation systems in the great plains with ERTS. Proceedings of the Third Earth Resources Satellite-1 Symposium (Maryland: NASA SP-351) 309 p.

Schimel, D.S., T.G.F. Kittel, A.K. Knapp, T.R. Seastedt, W.J. Parton, and V.B. Brown. 1991. Physiological interactions along resource gradients in a tallgrass prairie. Ecology 72:672–684.

Suyker, A. E. and S. B. Verma. 2001. Year-round observations of the net ecosystem exchange of carbon dioxide in a native tallgrass prairie. Global Change Biology 7:279–289.

Suyker, A.E., S.B. Verma, and G.G. Burba. 2003. Interannual variability in net CO_2 exchange of a native tallgrass prairie. Global Change Biology 9:255-265.

Villarreal, M., R.C. Cochran, D.E. Johnson, E.G. Towne, G.W.T. Wilson, D.C. Hartnett, and D.G. Goodin. 2006. The use of pasture reflectance characteristics and arbuscular mycorrhizal root colonization to predict pasture characteristics of tallgrass prairie grazed by cattle and bison. Grass and Forage Science 61:32-41.

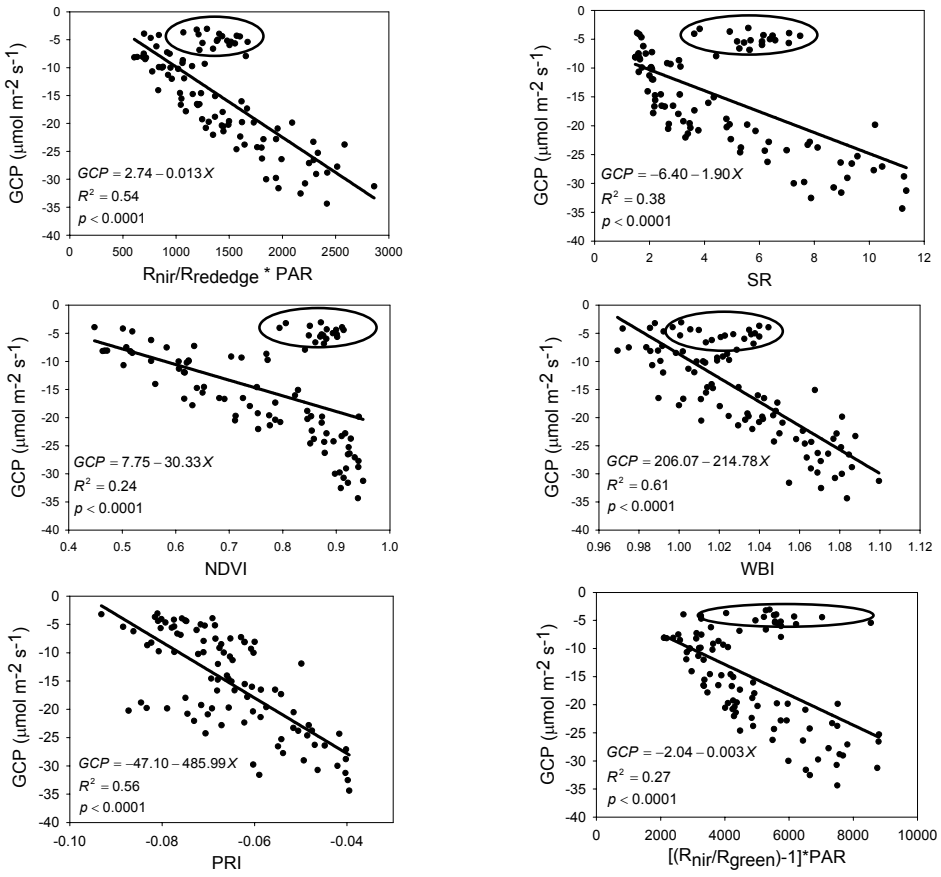

Figure 3.1. Relationships between [($R_{nir}/R_{rededge}$)-1] * PAR (a), the Normalized Difference Vegetation Index (NDVI) (b),the PRI (c), the Simple Ratio (SR) (d), the Water Band Index (WBI) (e), [(R_{nir}/R_{green})-1] * PAR (f), and Gross Canopy Photosynthesis (GCP) as determined by linear regression from June through October. The circled data points indicate the October 12th scans (n=99).

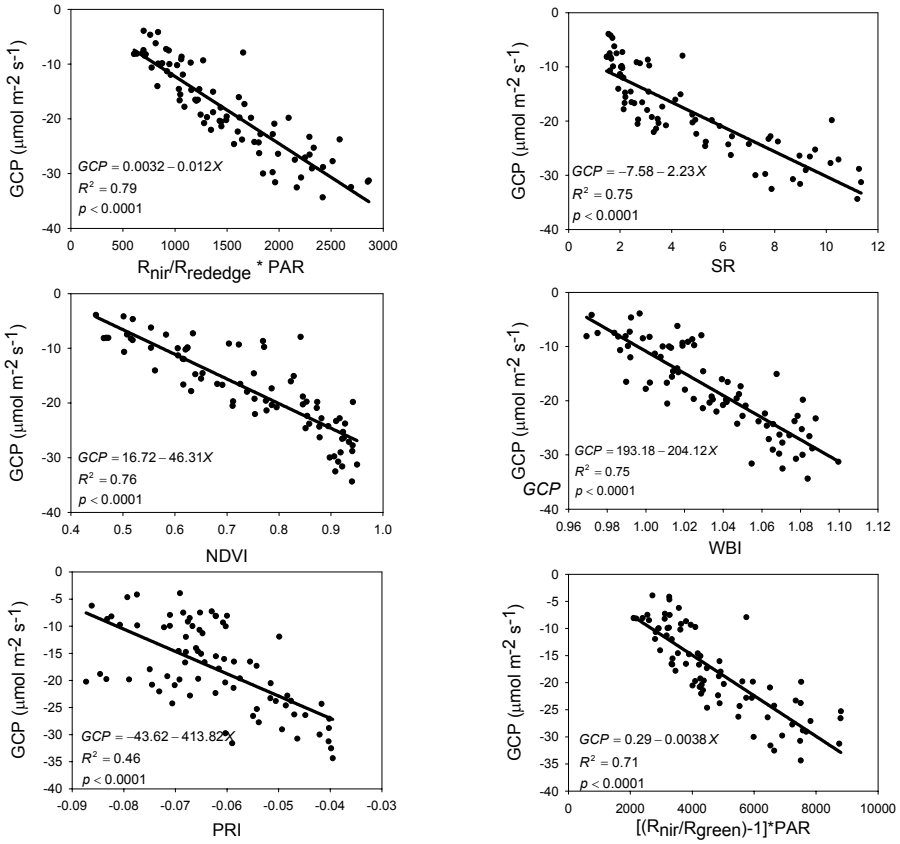

Figure 3.2. Relationships between [($R_{nir}/R_{rededge}$)-1] * PAR (a), Normalized Difference Vegetation Index (NDVI) (b), PRI (c), Simple Ratio (SR) (d), Water Band Index (WBI) (e), [(R_{nir}/R_{green})-1] * PAR (f), and Gross Canopy Photosynthesis (GCP) as determined by linear regression from June through September (n=81).

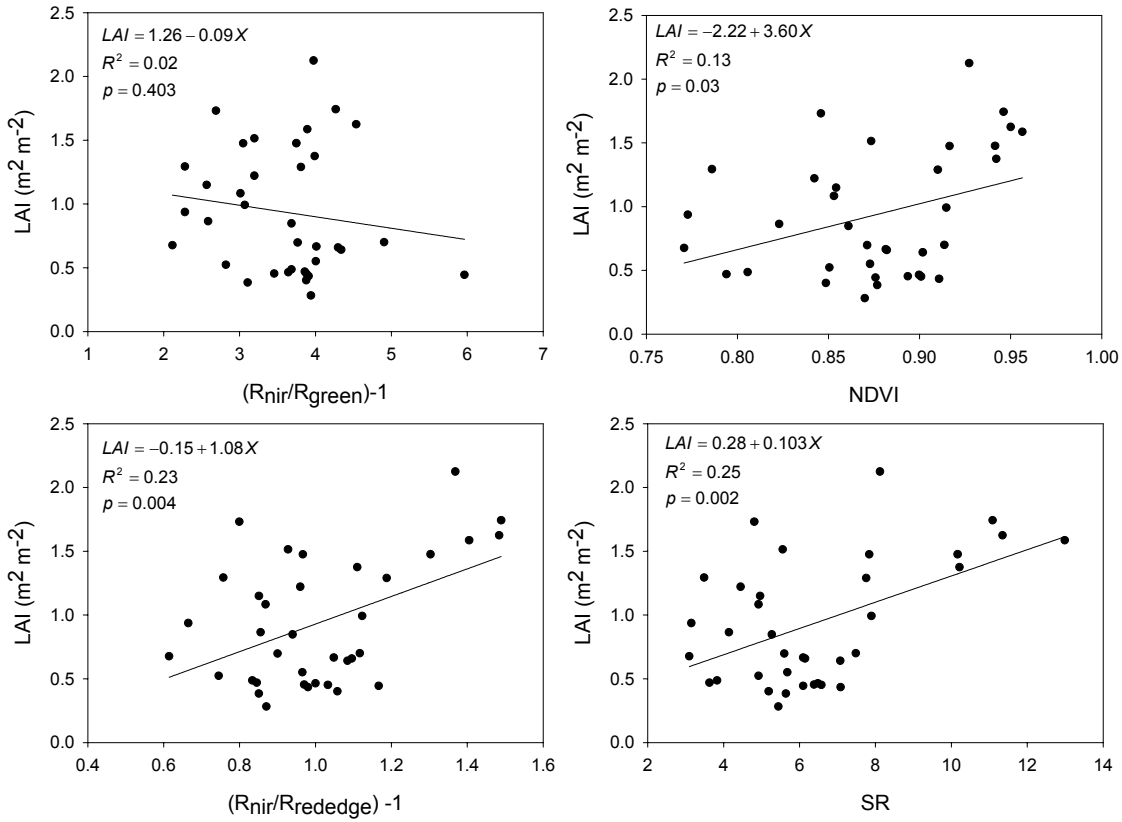

Figure 3.3. Relationships between (R_{nir}/R_{green})-1 (a), ($R_{nir}/R_{rededge}$)-1 (b), Normalized Difference Vegetation Index (NDVI) (c), Simple Ratio (SR) (d) and Leaf Area Index (LAI) as determined by linear regression from June through October (n=36).

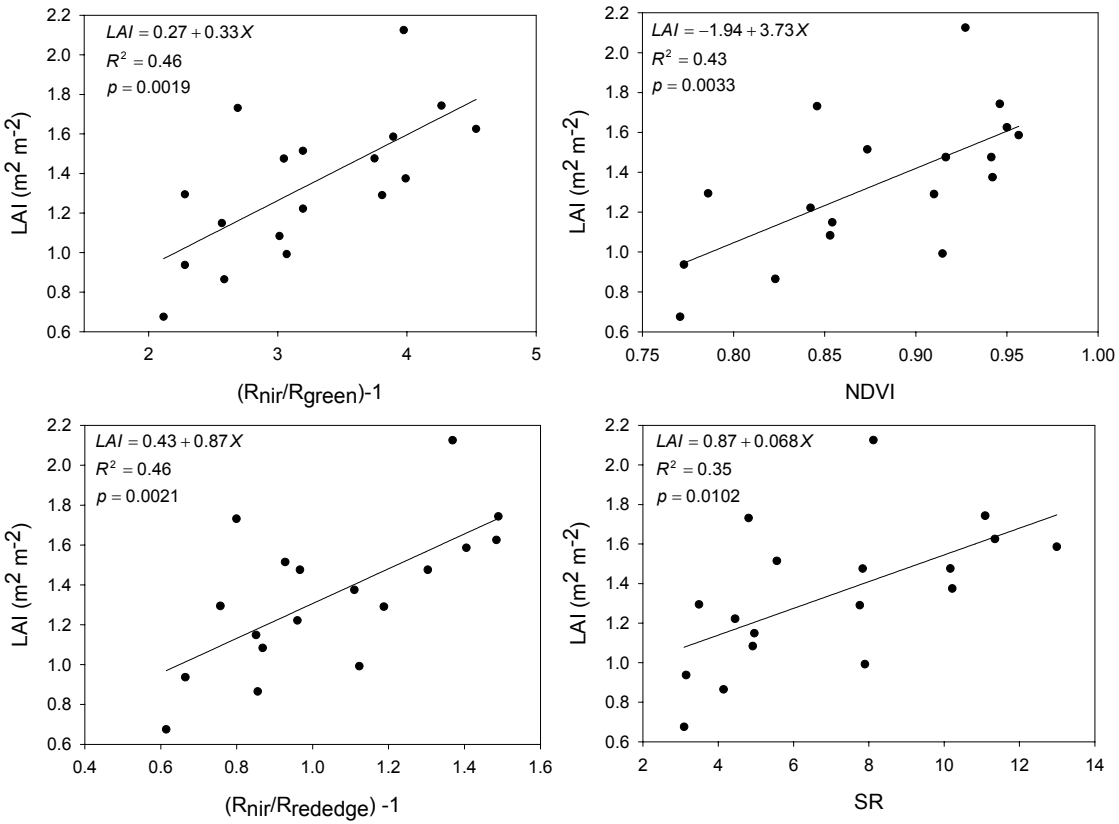

Figure 3.4. Relationships between (R_{nir}/R_{green})-1 (a), the ($R_{nir}/R_{rededge}$)-1 (b), Normalized Difference Vegetation Index (NDVI) (c), Simple Ratio (SR) (d), and Leaf Area Index (LAI) as determined by linear regression on data collect from June through August (n=18).

Table 3.1 Pearson's correlation coefficient for Gross Canopy Photosynthesis (GCP), Leaf Area Index (LAI), total biomass measured during either June 9 –October 12 (June-Oct), June 9 – August 16 (June-August) or June 9 – September 13 (June-Sept) and ($R_{nir}/R_{rededge}$)-1, NDVI, SR, WBI, (R_{nir}/R_{green})-1, and PRI vegetation indices and the number of hyperspectral scans (n).

	($R_{nir}/R_{rededge}$)-1	NDVI	SR	WBI	(R_{nir}/R_{green})-1	PRI	n
GCP *(June-Oct)*	-0.734***	-0.466***	-0.573***	-0.762***	-.0518***	-0.720***	99
GCP *(June-Sept)*	-0.905***	-0.872***	-0.868***	-0.865***	-0.845***	-0.676***	81
LAI *(June-Oct)*	0.469**	0.363*	0.498**	n/a	-0.144	n/a	36
LAI *(June-Aug)*	0.676**	0.654**	0.588*	n/a	0.680**	n/a	18
Biomass *(June-Oct)*	0.349*	0.192	0.305	n/a	-0.075	n/a	36
Biomass *(June-Aug)*	0.363	0.291	0.263	n/a	0.352	n/a	18

Correlations are significant at the 0.05 (*), 0.01 (**), and 0.0001 (***) levels. The n/a symbol indicates index was not utilized in comparison.